Pergamon

*Int. J. Multiphase Flow* Vol. 20, Suppl., pp. 261–295, 1994
Elsevier Science Ltd. Printed in Great Britain

0301-9322(94)E0025-E

# EXPERIMENTAL METHODS IN MULTIPHASE FLOWS

W. D. BACHALO
Aerometrics Inc., 550 Del Rey Ave, Sunnyvale, CA 94086, U.S.A.

*(Received 28 March 1994)*

**Abstract**—The research in the field of multiphase flows has been advanced as a result of the availability of optical diagnostics that allow the simultaneous measurement of the particle size and velocity of the dispersed phase. This capability also allows the measurement of the continuous phase turbulence parameters in the presence of the dispersed phase. The phase Doppler method has been a key method in providing this information. As an extension of the well-known laser Doppler velocimeter (LDV), it represents a major step in allowing the LDV instrument to be applied to the experimentation in multiphase flows. The phase Doppler method is described and the measurement characteristics are discussed along with the limitations of the method. Strategies for addressing these limitations which include the problems with high number densities and particle deformations are also presented. Evaluations of the measurement capability provide a credible measure of the instrument performance. The phase Doppler method is limited to the measurement of spherical particles, droplets or bubbles. In order to address the measurement of non-spherical particles, a new method based on near-forward light scatter detection is presented. This method utilizes the light scattering intensity to establish the particle size. The ambiguity that occurs as a result of random trajectories through the Gaussian beam intensity distribution is resolved with a confocal beam optical configuration along with a solution of the light scattering equations to obtain the particle trajectory through the beams. Because of the contemporary interest in the imaging methods, a brief discussion on the methods including particle imaging velocimetry (PIV) is provided. Although this method has not been extended to simultaneous particle size and velocity measurement, efforts are being made to reach this goal. The work concludes with some representative examples of the measurements in two-phase turbulent flows that are now possible. These measurements have been used to verify the drag coefficient and evaluate the particle response in turbulent flows. The particle interaction with large scale turbulent eddies has also been studied and some examples of these data are provided.

*Key Words:* phase Doppler particle analyzer, laser Doppler velocimeter, particle image velocimetry, light scattering, particle sizing, two-phase flows, turbulent two-phase flows, particle drag coefficient

## INTRODUCTION

The interaction of solid or liquid particles with turbulent flows, whether liquid or gaseous, represents one of the most interesting and challenging areas of research in fluid mechanics. Such flows are found in a wide range of applications including mixing in vessels for the chemical industry, transport of airborne particulates and in the mixing and combustion of fuels sprays. In addition to the challenges of understanding and predicting the continuous phase turbulent flow behavior in these flows, understanding and predicting the response of the particles adds another significant level of difficulty. Particles in the turbulent flow will respond in accord with their initial momentum and their inertia. In polydispersions, the particles will react to the various turbulent eddy sizes in accordance with the local Stokes number. It is well known that the interaction of particles with the large turbulent eddies provides an effective means for dispersing the particles.

The dispersion of the particles is not only limited to the large scale turbulent eddies, since the smaller particles will respond to the motion of the smaller turbulent structures. To what extent the various turbulent length scales play in the dispersion of the particles is a question that needs to be answered by careful experimentation. In high Reynolds number flows, the turbulence length scales as small as the particles may contain significant energy and will serve to disperse the smallest particles in the size distribution. The interaction can also create voids and clusters of particles. The clusters are formed by the accelerations and decelerations that occur as eddies form, interact and break-up. The particles, having a greater inertia, may tend to accumulate in the eddies or are centrifuged outward. The particles will also persist in maintaining their current velocities longer than the continuous phase.

Developing an understanding of the behavior of the particles in response to the turbulence has been and remains a challenge to the fluid dynamicist. Fortunately, significant advances in both the diagnostics and, consequently, the theory and computer modeling have occurred over the past decade. Early developments in the theory were hampered by a lack of reliable and detailed experimental data. As with the developments in continuous phase turbulent flows, the problem in modeling these flows lies, not so much in the numerics, but in the well-known turbulence closure problem. Unfortunately (or fortunately for the experimenters), all but the simplest second-order closure models require information from experiments to develop and validate the models. In many cases, and especially in the case of two-phase flows, the data on velocity fluctuations, Reynolds stresses, and other quantities have not been measured with sufficient detail and accuracy, if they have been measured at all. Moreover, the available data do not cover a sufficient range of conditions needed for the validation of the calculation methods. The predictive methods must deal with the fact that the turbulent two-phase flows are often inhomogeneous and anisotropic and usually involve mass, momentum and energy transfer between the phases. Furthermore, the dispersed phase may alter the structure of the turbulence as well as the continuous phase impacting the dispersed phase in the so-called two-way coupling. A serious problem is that modelers often forget that our description of the physical world must be based upon observations, and in scientific study, these observations are made through careful experimentation.

The evolution of laser diagnostics has played a tremendous role in making detailed and accurate experimental observations possible. The first significant invention was the laser Doppler velocimeter (LDV) in 1964 by Yeh & Cummins (1964). Even in its early form, this instrument was able to obtain very accurate measurements of particle motions in fluids. The discovery of this device by the fluid mechanics community pushed its development and application in a wide range of continuous phase flows. As with all diagnostics, the instrument was applied to progressively more difficult environments, including high speed flows. The velocity measurements of the continuous phase flows are dependent upon the presence of small particles in the flow that are capable of tracking the mean flow and turbulence-induced accelerations. In general, it was recognized that a means for simultaneously measuring the size and velocity of the particles would be of significant benefit in the study of a broad range of turbulent two-phase flows. Not only could the particle response characteristics be determined, but particles that are too large to reliably represent the continuous phase flow could be rejected (Farmer 1972; Durst 1982). Concern with the fidelity of these particles led to numerous efforts in developing the light scattering methods for particle characterization. Methods involving the measurement of the particle velocity response to sudden changes in the flow velocity, as may occur through a shock wave or on a stagnating streamline, were also used.

Other optical techniques, including the use of laser light sheets for direct imaging of the dispersed phase, are available to obtain detailed flow visualization and quantitative data. These methods provide instantaneous information of the spatial structures in the flow as opposed to the time-averaged point measurements of the LDV and phase Doppler method. One such method that is gaining acceptance in flow field measurements is the particle image velocimetry (PIV) method. This method utilizes a light sheet formed with a pulsed laser. Particles moving in a region of the flow field (typically $10 \times 10$ cm or smaller) are imaged at an instant in time using a double-pulsed laser with a suitable time separation between pulses for the prevailing velocity. The autocorrelation or cross correlation is used to resolve the flow velocity (magnitude and direction) based upon the separation between the images and the pulse separation. This approach provides an instantaneous record of the velocity vector field over the region allowing the qualitative and quantitative evaluation of the flow structures. Unfortunately, no method for simultaneous measurement of the particle size has been developed although several methods are being considered.

In the following sections, a brief description of a variety of optical measurement techniques will be provided along with a discussion on the range of reliability, accuracy and the limitations of the methods. Other non-optical multiphase measurement techniques have been described elsewhere, for example, O'Hern & Gore (1991). Problems associated with the simultaneous measurement of the continuous phase and the dispersed phase will be reviewed. Techniques will also be described for measuring the local particle concentration, including the time dependent fluctuations of the velocity and concentration. Methods derived for measuring the mixing of two

turbulent flows will also be described. Some examples of the experimentation that is now possible in multiphase flows are provided.

## METHODS FOR SIMULTANEOUS PARTICLE SIZE AND VELOCITY MEASUREMENTS

### *Measurement Environment and Associated Problems*

Early efforts in applying the LDV combined with a particle sizing approach failed, in most part, due to the high particle concentrations that exist in most practical two-phase turbulent flows. The original optical configurations were believed to be limited to confocal on-axis light scatter detection. This resulted in the formation of a rather large sampling or probe volume. For the proper performance of these single particle counters, there must be a high probability of only one particle residing in the sample volume at one time. In dense particle fields, this can only be accomplished if the sample volume is very small. To cope with this problem, large off-axis light scatter detection angles and highly focused laser beams were used by Bachalo (1980). For example, current phase Doppler instruments are designed with a sample volume that may be smaller than the largest particle to be measured. Thus, the coincidence problem no longer represents the serious limitation that previously prohibited the application of these single particle counters in dense particle environments.

The other limitation on the particle number densities within which these instruments will function is determined by the laser beam extinction. The beam extinction is given by the Beer–Lambert law as:

$$\text{ext}(x) = 1 - \exp\left[ -\int_{y1}^{y2} \tau\,(x, y)\,\mathrm{d}y \right]$$

where $\tau\,(y)$ is given by

$$\tau\,(y) = \text{ND}(y)\,\frac{\pi}{4}\,Q\,(d_{20}(y))^2$$

in which $y$ is the variable representing the optical path, $\text{ND}(y)$ is the number density distribution along $y$, $Q$ is the extinction coefficient and $d_{20}$ is the area mean diameter. Beam extinction can be seen to depend upon the particle size distribution, the number density, optical path length through the medium and the light scattering efficiency which approaches 2 for particles larger than approx. 20 $\mu$m. It is possible that the single particle counting instruments may still function even if the beam extinction is as high as 80% provided that the initial laser power is high enough. However, robust signal processing methods are required to ensure that the signals from the smallest particles are detected and reliably processed. Because of the beam intensity fluctuation that will occur due to larger particles passing the beams near the sample volume, intensity fluctuations at the sample volume may be significant and the beam coherence will be adversely affected. For approaches such as the phase Doppler method that are based on light scattering interferometry, the measurements of the particle size and velocity will not be affected by the fluctuations in the light scattering intensity. Methods developed to overcome the corresponding problems associated with the loss in signal-to-noise ratio (SNR) will be described.

Measurements in two-phase flows implies the need to obtain data on the continuous phase mean and turbulence quantities without interference from the dispersed phase. When applying the laser Doppler or phase Doppler methods, the measurements are made by analyzing the light scattered by small particles in the flow that will respond to the mean flow velocity accelerations and to the turbulent velocity fluctuations. Particles on the order of 1 $\mu$m are required to reliably resolve the flow velocities. This requirement is especially true if the Reynolds number is high and there are accelerations and decelerations in the flow. These measurements must be made in the presence of the dispersed phase which may consist of particles as large as 500 $\mu$m or larger. Since the particles scatter light approximately in proportion to their diameter squared, the amplitude dynamic range requirement for the photodetectors and the preamplifiers will be as great as $25 \times 10^4$. Fortunately, the light scattered by particles larger than a few microns produce signals with a good SNR so it is possible to simultaneously measure the particle size and velocity over a dynamic size range of

50–1 or greater. For size ranges larger than this, the sizing capability may still be used to discriminate between the small seed particles that will track the continuous phase flow and the larger dispersed phase particles.

*Laser Doppler velocimeter (LDV)*

The laser Doppler velocimeter has been the most productive instrument in fluid dynamics research. As a result of three decades of development, the instrument has become very reliable, accurate and easy to use. The method is described in numerous articles (Adrian *et al.* 1990; Durst *et al.* 1981; Bessem *et al.* 1993), and thus, does not need to be described here. The laser Doppler method has been demonstrated as being able to accurately measure flow velocities, based on the velocity of small seed particles in the fluid, over a velocity range from creeping to hypersonic flows. The measurements are made *in situ* and non-intrusively in flow fields that range in size from less than a millimeter to many meters in cross section. The primary problem with the application of the standard LDV to multiphase flows is that the instrument cannot reliably discriminate between the seed particles that represent continuous phase flow and the larger particles of the dispersed phase.

Prior to the development of the phase Doppler approach, the LDV was applied to the measurements of turbulent two-phase flows using signal amplitude discrimination to separate signals generated by the dispersed phase from signals generated by the seed particles (Modarress *et al.* 1982). However, these early attempts produced questionable results due to the contamination of the continuous phase flow measurements with velocity readings from the dispersed phase particles. The problem was simply that the signal amplitude varied with the particle trajectory through the Gaussian intensity beam, in addition to the amplitude variation that is proportional to the particle size. Thus, simple signal amplitude discrimination allowed some of the larger particles which passed through the low intensity edge of the beam to be accepted, even though they were not small enough to track the continuous phase turbulent flow.

## *Measurement of Spherical Particle Dynamics: Phase Doppler Method*

*Description of the concept*

The requirement of sizing particles with high accuracy over a large size range in low to high particle number density environments suggested the utilization of the light scattered at large off-axis angles. Light scattered at these angles is dominated by the mechanisms of reflection and refraction rather than by diffraction as in the case of on-axis scattered light detection. The angular distribution of the light scattered by reflection and refraction is independent of the drop size except for the higher frequency resonant structure on the scattering intensity distribution which is produced by the interference between the light scattering components. The light scattered at angles away from the forward direction (greater than 20°) is used to avoid the light scattered by Fraunhofer diffraction. A detailed treatise of this and other characteristics of the light scattering phenomena is given by van de Hulst (1981).

A basic theory for dual beam light scattering and interference was derived by Bachalo (1980) which indicated that the phase shift of the light scattered by refraction or reflection from two intersecting laser beams could be used to size spherical particles. Based on the analysis given by van de Hulst, the optical path length of a light ray passing through a sphere, relative to a reference ray deflected at the center of the sphere, is given as

$$\eta = 2\alpha\,(\sin\tau - pm\sin\tau')$$

where $\alpha$ is the size parameter ($\alpha = \pi d/\lambda$), $m$ is the index of refraction of the particle relative to the medium, $\tau$ and $\tau'$ are the angles between the surface tangent and the incident refracted rays, respectively, and $p$ is a parameter that characterizes the emerging rays and relates to the interface from which it emerges. For example, $p = 0$ for first surface reflection, $p = 1$ for the transmitted ray and $p = 2$ for the ray emerging after one internal reflection.

The phase shift is obtained using light scattering interferometry produced with a dual beam LDV. With this optical configuration, the light rays from each beam are incident upon the particle at different angles and therefore reach common points on the receiver via different optical paths. By

neglecting the phase shifts at reflection and focal lines, the relative phase shift due to the differing optical paths is described as

$$\phi = \frac{2\pi d}{\lambda}[(\sin\tau_1 - \sin\tau_2) - ipm\,(\sin\tau_1' - \sin\tau_2')]$$

where the subscripts represent beams 1 and 2. Since the angles $\tau$ are fixed by the receiver geometry, the phase difference only changes as a result of the particle diameter, $d$. These phase differences produce an interference fringe pattern that can be analyzed to obtain the size and velocity of spherical particles. The temporal frequency of the interference fringe pattern occurs as a result of the Doppler difference frequency scattered by a moving particle simultaneously from beams 1 and 2, and is a function of the beam intersection angle, laser wavelength and the velocity of the particle. The spatial frequency of the fringe pattern, which is linearly related to the beam intersection angle, laser wavelength, angle of observation and particle index of refraction (unless reflected light is used), is inversely proportional to the particle diameter. With the complete description of the interference fringe pattern produced by the scattered light for the appropriate optical parameters, there is no longer any need to calibrate the system for each measurement task. Normally, calibration is only needed to accurately define the settings of the optical system including the beam separation angles and the effective detector separations in the receiver. The particle size measurement can subsequently be obtained from the accurate measurement of the spatial frequency of the interference fringe pattern.

A direct means of measuring the interference fringe pattern based on the approach first described by Crane (1969) was developed by Bachalo & Houser (1984a). The scheme uses pairs of detectors located at known angles with respect to the laser beams, and separated by fixed spacings. As a particle passes through the beam intersection region, it produces a scattered interference fringe pattern that appears to move past the receiver at the Doppler difference frequency. Doppler burst signals are produced by each of the detectors at the same frequency but with a phase shift between them. The frequency and phase shift between the signals can be measured using a number of methods, with the Fourier transform approach offering the optimum method (Ibrahim *et al.* 1990).

Measurements of the phase shift are then related to the particle size using the linear relationships derived from the theoretical calculations or from experimentation using known-sized monodispersed particles. An example of the phase diagram for a three detector system is shown in figure 1. In this figure, the effect of changing the optical parameters, which include the laser beam intersection angle, collection angle, drop index of refraction, laser wavelength and the light scattering component detected, is to simply change the slope of the linear response curves. That is, only the size scale is changed for the same range of phase angles, since all curves must pass through the origin.

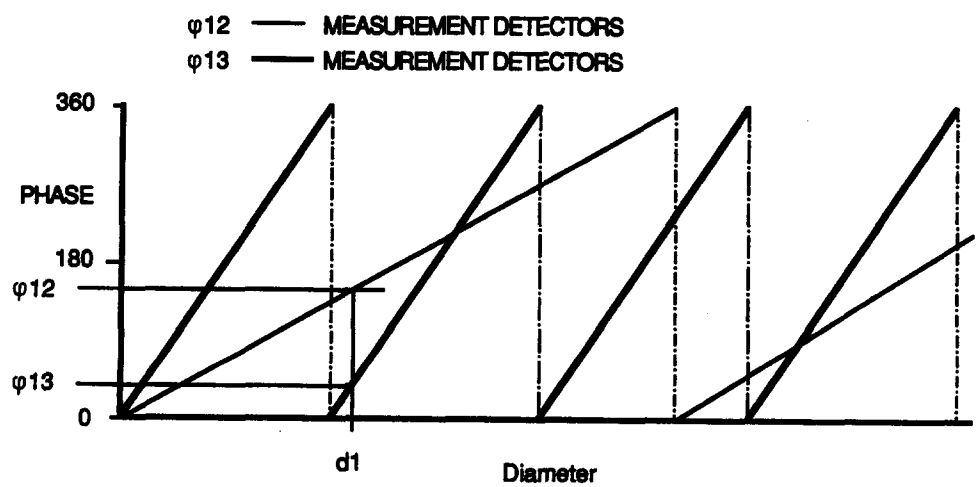


Figure 1. Phase diagram for a three detector PDPA system.

Three detectors are used to extend the size range and maintain a high resolution since phase measurements over several cycles are possible. The two pairs of detectors also serve as redundant measurements for additional testing of the signals and to extend the size range sensitivity at one optical setting to any desired value. However, the particles scatter light in proportion to their diameter squared so the required detector response is more than $10^4$ for a size range of 50–1. This large amplitude dynamic range and the signal-to-noise ratio is the reason for the limitation on the dynamic particle size range.

More recent investigations of the phase Doppler method have used more advanced analysis based on both geometrical optics and Lorenz–Mie scattering theory to reveal some of the subtleties leading to possible uncertainties in measurements if appropriate measures are not taken in the optical and electronics system design (Sankar & Bachalo 1991; Grehan *et al.* 1992).

*Effects of particle trajectory through the Gaussian beams*

The phase Doppler method is not as ideal as the simple analysis described above might indicate. Although the detection of a single light scattering component (either reflection or refraction) is expected, on certain trajectories through the focused Gaussian beams, large particles may scatter significant light by the wrong mechanism. For example, the 30° light scattering angle was selected to minimize the contribution of the reflected light when measuring transparent spherical particles. At this angle, the intensity of the light scattered by refraction is approx. 80 times greater than that scattered by reflection, assuming uniform illumination. Unfortunately, more highly focused laser beams are required when attempting to make measurements in high particle number density environments to ensure a high probability of only a single particle residing in the sample volume at one time. This requirement will result in the non-uniform illumination of the larger particles, as shown in figure 2. For larger particles (diameters approaching the beam waist diameter), the particle trajectory through the beam can significantly influence the balance between the light scattering components. This problem was considered by Bachalo & Houser (1984b) and by Saffman (1986).

The effect of the trajectory-dependent non-uniform illumination on the light scattering and phase response can be determined using the geometrical optics theory developed by Sankar & Bachalo (1991). This theory accounts for the first surface reflection, the refraction and up to two internal reflections. Effects of random trajectories through the Gaussian intensity distribution of the focused

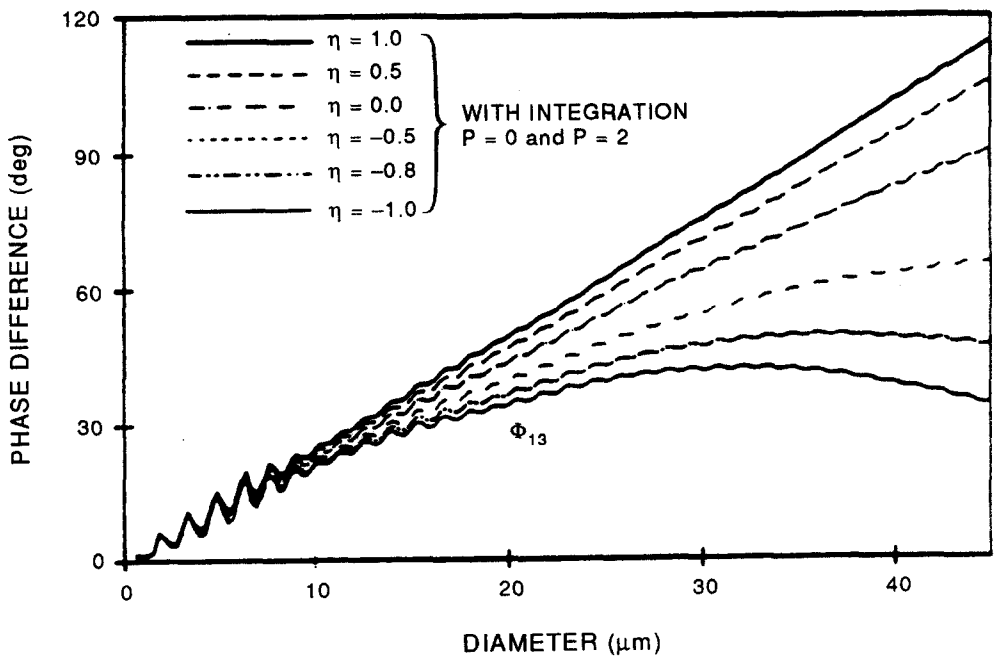


Figure 2. Trajectory-dependent light scattering, $\eta = x/b_0$.

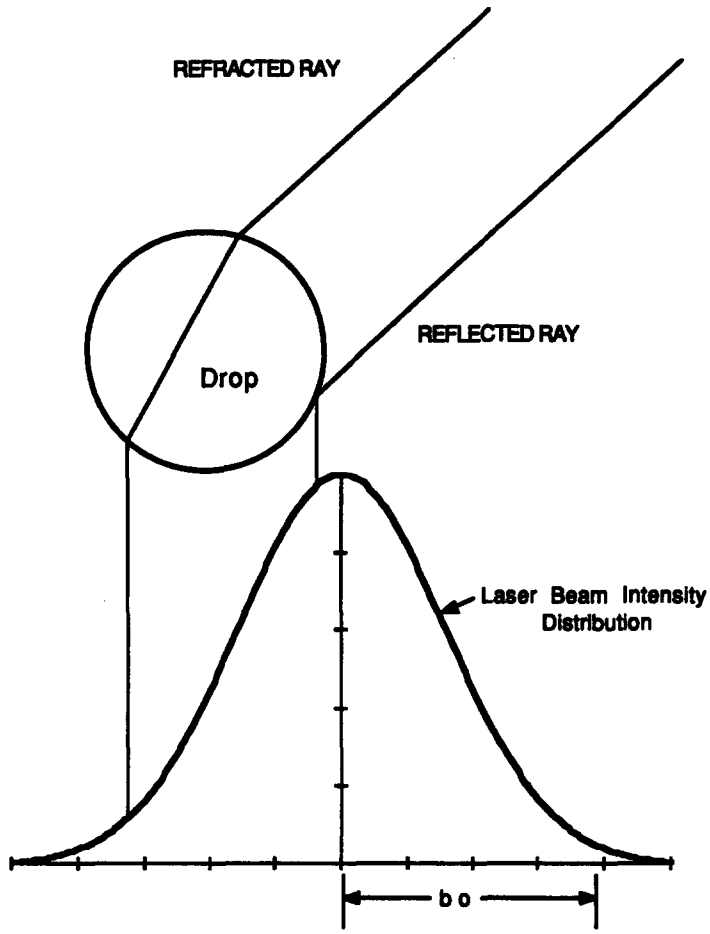


Figure 3. Trajectory dependence of the phase response for a mean light scattering angle of 30°.

laser beam were described by imposing the intensity distribution centered at different radii. In addition, the temporal variations in the light scattering intensity and phase were described as the particle passes through the beam. Examples of the trajectory-dependent scattering are shown in figure 3. Detection of the wrong light scattering component can lead to serious measurement errors. The extent of these errors has been shown by Sankar *et al.* (1991). In this figure, $\eta$ is the dimensionless coordinate describing the particle trajectory through the beam ($\eta = 1$ is when the trajectory is at the $1/e^2$ radius).

The use of three detectors (Bachalo & Houser 1984c) was suggested as one method for rejecting the light scattered by the undesired scattering component. This approach helped reduce errors, especially if the undesired scattering component was dominant, as in the special case of particles as large or larger than the focused beam diameter passing on a trajectory wherein the peak intensity falls on the point where the light is reflected to the receiver. However, particles of a full size range and all possible trajectories will occur in real spray measurements. In this case, the approach of comparing the phase measurements between the two pairs of detectors generally failed. The approach failed because the change in the phase continuously deviates from the ideal linear response instead of simply switching from either positive or negative, depending on whether the light scattering was by refraction or reflection.

The problem became serious when it was necessary to probe dense sprays, such as those produced by rocket, gas turbine or diesel injectors. In these cases, the sample volume diameter must be made as small as possible to ensure a reasonable probability that only one particle will reside in the sample volume at one time, whereas the particle size range is relatively large. Under this constraint, the particle-to-probe volume diameter ratio will increase, making the system more susceptible to the errors associated with the trajectory dependent scattering.

Several approaches have been used to analyze this problem. Gouesbet *et al.* (1990) developed the generalized Lorenz–Mie theory (GLMT) to extend the Lorenz–Mie theory to account for the non-uniform illumination of drops. Although the GLMT is a significant contribution in delineating the light scattering from non-uniformly illuminated particles, it is not generally required for describing the light scattering involved in the phase Doppler method. By comparisons of calculations with similar optical parameters, it was shown that the results procured with the GLMT theory agreed with the results obtained with the theory of Sankar and Bachalo.

An important contribution of Sankar *et al.* (1992) was the observation that the trajectory dependent errors could be minimized with a proper selection of the optical configuration. Specifically, when two laser beams intersect and a particle scatters light from each beam simultaneously, the resulting interference pattern depends not only upon the individual amplitudes of the light scattering components, but also upon their relative phases. By changing the beam intersection angle, the phases of the reflecting and refracting light scattering components are also changed. This approach was used effectively to decrease the error resulting from the trajectory effect. For example, by changing the beam intersection angle from 1.8 to 5.4° (figure 4), the sizing error of the 45 $\mu$m particle decreased from 50% to approx. 10% for trajectories creating the greatest errors. It should be emphasized that only a small percentage of the particles passing through the probe volume will pass on this trajectory.

This error may be reduced further with the use of two pairs of measurement detectors as introduced by Bachalo & Houser (1984c) for phase validation. Although it was stated earlier that the method is not completely effective in eliminating the problem, it is useful as one of several methods for eliminating serious errors produced by particles passing on particular trajectories. The most effective approach is to combine this with the use of the light scattering intensity to limit the acceptance of particles that pass on trajectories near the edge of the beams. In this approach (Bachalo 1989) a minimum admissible light scattering intensity was set for each particle size in the range of interest. The method may be considered as having a separate threshold level for the detection and acceptance of each particle size class (figure 5). Since the light scattered by reflection is almost two orders of magnitude less than that scattered by refraction (assuming the correct polarization is used), the scattering intensity serves as a very effective means for eliminating these signals. Particles that pass on trajectories through the edge of the beam nearest the receiver and scatter light dominated by refraction are also eliminated. This is advantageous as these particles will produce signals with lower signal-to-noise ratio, but more important, the diameter of the sample volume is better-defined when these edge trajectories are eliminated. Consequently, the number density and volume flux measurements were improved. The intensity validation has been

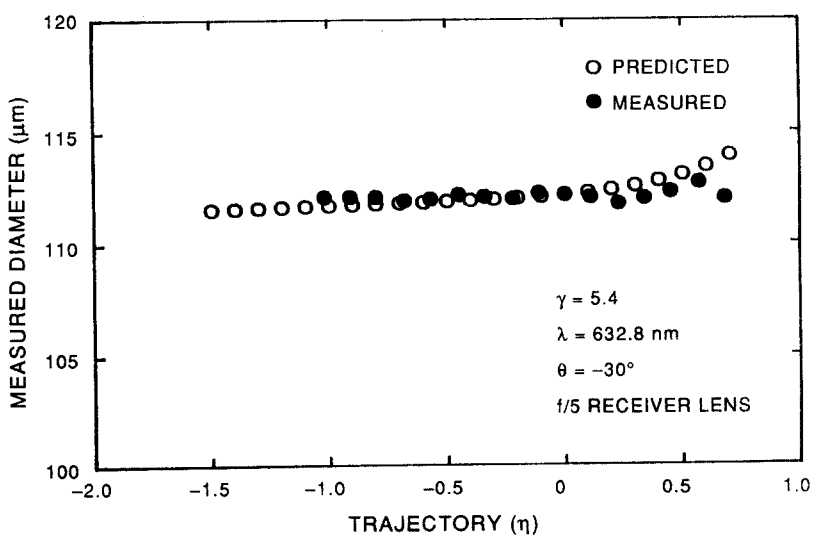


Figure 4. Measured and predicted variation of measured particle size with particle trajectory for a particle diameter of 0.64 × probe diameter.

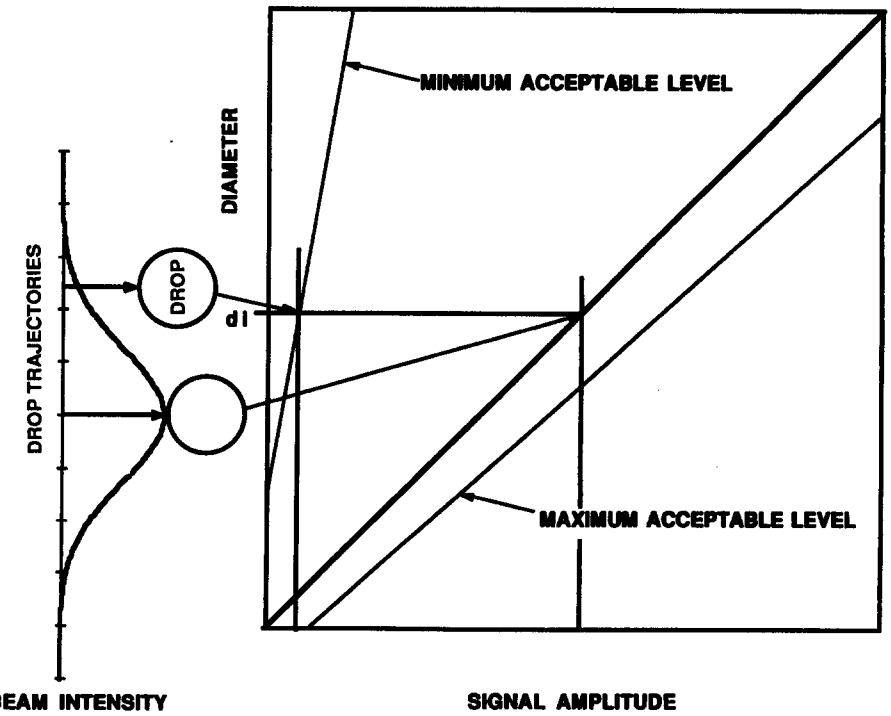


Figure 5. Signal amplitude validation used to reject PDPA signals from particles grazing the edge of the probe volume.

demonstrated to be highly reliable in eliminating the erroneous measurement of particles scattering light by reflection when refraction was expected. The adverse effects of the particle trajectories have been minimized with these and other improvements.

*Particle number density limitations*

The phase Doppler method is capable of accurately measuring the particle size distribution and velocity. In addition, the particle number density and volume flux can also be determined. However, these measurements, especially the number density, will begin to fail if the particle concentration is too high. Single particle counters must have a sample volume that is small enough such that the probability of more than one particle passing the probe volume at one time is minimized. Otherwise, the particles will be rejected which results in errors in the particle count. The use of large off-axis light detection angles significantly improved the performance of single particle counters in dense sprays because of the tremendous reduction in the size of the sample volume as compared to near forward or backscatter light detection. If the particle concentration is too high, occurrences with more than one particle passing the sample volume will increase.

A recent detailed analysis of the problem was presented by Edwards & Marx (1992). The authors assumed an ideal system in the analysis in which all-coincident occurrences were rejected by the instrument. Two Poisson filters were applied, one for the spatial distribution of the particles and a second for the temporal or arrival time statistics. Since the size of the sample volume will be different for different particle sizes, the analysis also accounted for this change in sample volume. The particles are assumed to be distributed randomly and homogeneously in space and have a number density $\rho$. In order for a particle to be measured successfully with the ideal system, the particle must not be accompanied by any other particles during its passage through the sample volume. Under these conditions, the analysis of Edwards and Marx indicated that the particle must pass both the spatial and temporal filters. The probability of passing the spatial filter was given as:

$$P_x = e^{-\rho V}$$

where $V$ is the size of the measurement volume and $\rho$ is the particle number density. The probability that no other particle enters the probe volume during the transit time, $t = D/v$ of the particle being measured is the probability of passing the temporal filter:

$$P_t = e^{-\delta t}$$

The combined probability for a successful measurement is just the joint probability expressed as

$$P = P_x P_t$$

The possible difference in velocities between the various size classes requires the temporal filter. The spatial Poisson process rejects particles resulting from insufficient spacing, whereas the temporal Poisson process rejects particles for excessive residence times.

The analysis of Edwards & Marx indicated that for an ideal system, the mean drop size and, particularly, $D_{32}$ would not be reported with significant error even with a low probability for acceptance of the measurements. Only the particle number density and volume flux would be in error. This follows from the assumption that the rejection does not depend upon the size of the particle except the larger particles are detected over a larger sample volume.

In reality, the instrument is imperfect because it may not reject all coincident occurrences. Logic systems including redundant phase measurements, signal-to-noise ratio checks, and signal amplitude measurements are all incorporated into the more advanced commercial instruments to prevent erroneous measurements. However, it is possible that coincidental events may be accepted and produce errors. For example, if a large and a small particle are resident in the sample volume at one time, the signal from the large particle will dominate and may be successfully measured. In other cases, particles of nearly equal size may pass with approximately the same velocity (Doppler frequency) and phase, and may also be accepted. The performance of the PDPA under conditions of two particles passing the sample volume at one time is described in Sankar *et al.* (1994).

Recent developments in signal processing have led to the capability of measuring the signal at very high rates using the Fourier transform. Given this exceptional processing speed, these advanced methods present the possibility of measuring segments of the signal and evaluating the frequency, phase and signal-to-noise ratio for each segment. When more than one particle occurs in the sample volume at one time, it may be possible to separate the two events, provided that the signals do not completely overlap in time. This separation is possible using the Fourier transform processors, Sankar *et al.* (1994).

*Particle flux and number density measurements*

The local particle number density and volume flux are important parameters in the study of particle dispersion in multiphase flows. Accurate measurements of these quantities are important to the understanding of the mixing processes and the development of the predictive models. The phase Doppler method has the potential of measuring these quantities with sufficient accuracy. In addition, it can measure the time varying nature of these parameters which will result from the interaction with the large scale structures in the flow. Early attempts at measuring the number density and volume flux showed mixed success; in some cases the measurements were shown to be accurate (Dodge *et al.* 1986; McDonell *et al.* 1987; Bachalo 1987), and in other cases, the results were shown to be in error. An example of some reliable results are shown in figure 6.

Several reasons for the inconsistent measurements of the number density have been identified. In some cases, the non-uniformities in the spray distribution being measured resulted in the point measurements of the phase Doppler method differing from the line averaged methods to which it was compared. In other attempts, the swirl and reversed flows within the spray presented problems in the determination of the sample volume size determination when only a single component of velocity was measured (Zhu *et al.* 1993). The presence of relatively large particles in the spray drop size distribution have also caused momentary attenuations to the laser beam intensity. Consequently, the signal burst detection system would count a significant number of single particle events each as several particles. Finally, in high particle number density flows, the beam extinction results in the loss of the counting efficiency of the small particles in the distribution. Each of these problems have been addressed in the recent developments of the instrumentation.

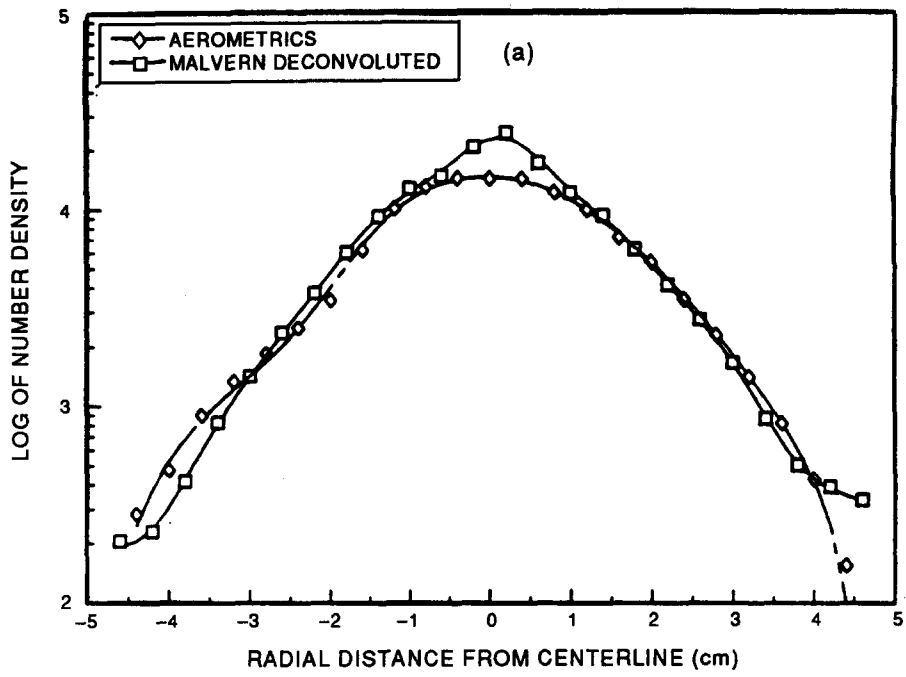


Figure 6. Comparison of the number density measurements obtained from PDPA and Malvern instruments (from Dodge *et al.* 1986).

Reliable measurements of the number density and volume flux depend directly upon the accuracy to which the size of the sample volume can be determined. Since the laser beam intensity profile is Gaussian, and particles scatter light in proportion to their diameter squared, the effective size of the sampling volume will change with particle size. A means for measuring this change in probe volume size, and correcting for the statistical bias that it produces, has been incorporated into the commercial instruments (Bachalo & Houser 1984b). Determination of the probe diameter for each size class depends upon the measurement of the transit time and velocity statistics of each particle size class that passes the sample volume. This establishes the probe volume, $V_i$ for each size class and the effective probe area (Zhu *et al.* 1993). The number density is then determined from the expression

$$\rho = \frac{1}{t_T} \sum_i \frac{\sum_j}{t(i,j)} V_i$$

where $t_T$ is the total time for the sample accumulation and $t(i,j)$ is the transit time of the $i$th particle of size class $j$. It should be recognized that multiple triggering on individual particles passing the probe volume (due to momentary extinctions of the beam caused by large particles passing through and blocking the beams prior to the sample volume) will not have the same serious effect as with the earlier methods. The volume flux is a vector quantity. The scalar flux or magnitude is measured as

$$V_f = \frac{\pi}{6} \frac{ND_{30}^3}{6t_T PA}$$

where $N$ is the number of particles in the sample, $D_{30}$ is the volume mean diameter and $PA$ is the probe cross sectional area.

The number density problem associated with non-uniformities in the particle field was relatively easy to resolve. In such cases, more radial distributions at different azimuthal angles must be acquired. This provides information on the spray pattern, for example, and allows the evaluation of the accuracy of the volume flux and number density distributions using comparisons to flow rate and line of sight extinction measurements.

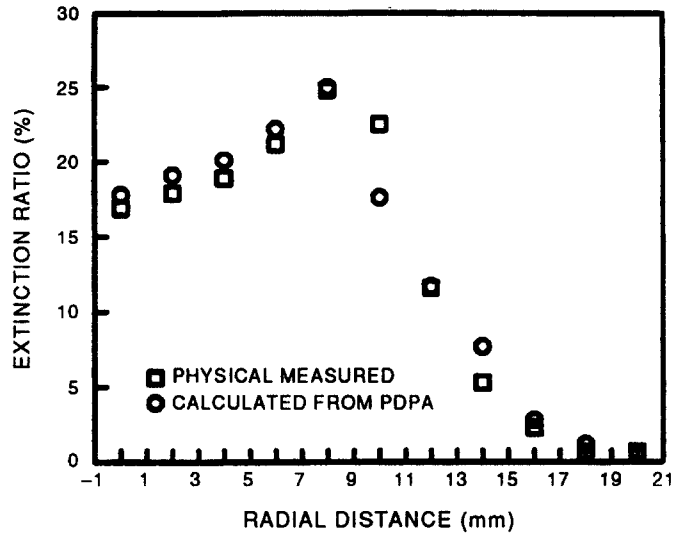


Figure 7. Comparison of the number density measurements obtained from PDPA and the extinction method (from Zhu *et al.* 1993).

To demonstrate the performance of the most recent methods which included an innovative Fourier transform signal burst detector and processing method (Ibrahim & Bachalo 1992), a comparison of the number densities measured with the phase Doppler instrument to that given by the extinction method is shown in figure 7. For this simple case of spray drops generated by a pressure atomizer, the agreement was very good. When there is a high degree of swirl or recirculation, the results are less accurate but are estimated to be within $\pm 15\%$ of the true value. New methods for defining the sampling cross-section are under development and show promise in further improving the measurement accuracies in complex swirling turbulent flows with recirculation.

*Time-dependent flow measurements*

A very important feature of the phase Doppler method, or other single particle counting methods, is the ability to provide a time record of the particle size and velocity measurements. Time-resolved measurements of the dispersed and continuous phase velocities, for example, can provide information on the local slip or relative velocity between the particles and the continuous phase. The slip velocity will impact the heat and mass transfer between the particle and the fluid, for example. The time-dependent response of the particles can also be used to infer the mixing efficiency in both the small and large scale turbulent motions. For example, in a highly seeded flow, a nearly continuous record of the turbulent velocity fluctuations may be obtained. Within this time record, the dispersed phase particle size and velocity are measured. The differences in the velocities between the continuous phase and the dispersed phase are then used to infer the slip velocity.

Particle time of arrival statistics may be used to discern whether any clustering or other unsteadiness exists in the dispersed phase. The phenomena of clustering may be recognized as unsteady groupings of particle arrivals in the particle time-of-arrival records. Using the widowing approach described above, the discrete Fourier transform of the particle arrivals may be applied to detect any periodicity in the particle arrivals. The arrival rates may, however, show clustering but the cluster formation is not periodic as for example in the case of a turbulent flow wherein the particles are accumulating in eddies of various length scales. In such cases, the detection of the clusters becomes more difficult and requires sophisticated analysis (Edwards & Marx 1994).

*Particle shape effects*

Multiphase flow research may require the measurement of particles that are not spherical or even quasi-spherical. Non-spherical particles may be classified into two types; those that are irregularly-

shaped solid particles, such as sand, powders, sugar, etc. that have facets and sharp edges and those that are liquid particles or drops that have been disturbed from spherical by pressure or shear forces to form, for example, prolate and oblate spheroids. The irregular particles may be expected to produce highly irregular light scattering patterns. The reflected or refracted light will depend on the shape of the surface from which the light is reflected or through which it is refracted to the receiver. Such irregular particles cannot be measured reliably using the phase Doppler method. Using three detectors, the two-phase measurements may be used to discriminate against a high percentage of the irregular particles, although some erroneous readings may be accepted. The probability of these irregular particles passing this test is very low.

Most often, the phase Doppler method is applied to the measurement of spherical particles, such as spray drops or bubbles. The surface tension in these applications provides a relatively strong restoring force to maintain the sphericity of the drops. This is true for small drops but for drops on the order of 100 $\mu$m or larger, in the process of forming or under aerodynamic loads induced by flow accelerations and turbulence, the drops may deviate from spherical. The deviation from spherical for liquid particles under steady state aerodynamic deformation can be estimated as (Hinze 1947)

$$\left(\frac{2\delta}{d}\right)_{\max} = -0.095\rho\frac{d}{2}\frac{U_r^2}{\sigma}$$

where $\delta$ is the radial displacement of the droplet surface from its position in the undeformed state, $\rho$ is the density of the air or surrounding fluid, $U_r$ is the relative velocity between the fluid and the drop and $\sigma$ is the drop surface tension. In the case of impulsive deformations due to turbulence etc., the deformation is estimated as

$$\left(\frac{2\delta}{d}\right)_{\max} = -0.17\rho\frac{d}{2}\frac{U_r^2}{\sigma}$$

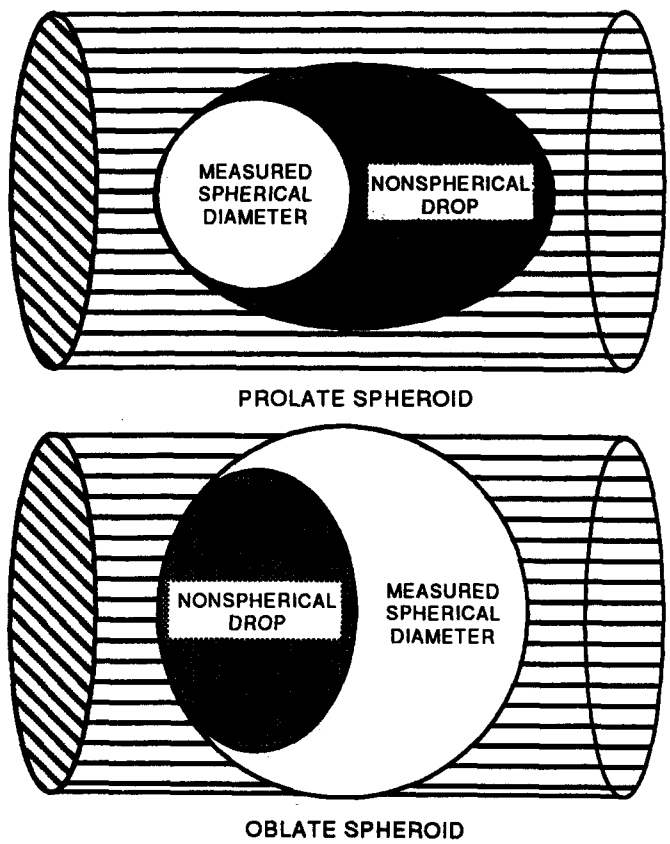


Figure 8. Schematic showing the response of the phase Doppler method to non-spherical particles.

which is approximately twice that of the steady state case. The drop size measurements in such cases will have an error that depends upon the degree of the distortion.

The phase Doppler method responds to the local radius of curvature of the particle. For refractive light scattering, the radius of curvature of the entering and exiting light that reaches the detectors affects the response. Furthermore, it is primarily the radius of curvature in the plane of the two incident beams (figure 8) that is most significant to the measured result. Thus, the measurement error also depends upon the orientation of the drop, as well as its shape. It may be argued that if the distorted drops are randomly orientated or oscillating, the average size will adequately represent the equivalent sphere. If the drops are preferentially distorted as might be the case when the aerodynamic forces of an accelerating or decelerating flow are experienced, then an error will result. For such conditions, a system with multi-directional measurements has been developed so that, an approximate shape factor can be measured. This approach works if the distortions to the sphericity lead to a regular shape, such as a prolate or oblate spheroid.

Using two pairs of detectors will not detect this asphericity since the radius of curvature is regular over the region of the drop that scatters light to the receiver. Thus, the two-phase measurements will be consistent with that of a sphere. The asphericity can be detected if two pairs of incident beams in planes orthogonal to each other are used with two receivers located at the suitable angles.

A basic study showing the measurement error for drops having different aspect ratios (major and minor axis lengths) was conducted experimentally by Alexander *et al.* (1985). In this study, a monodispersed drop generator was used to produce oscillating drops of a known spherical diameter. The phase of the drop oscillation is fixed in space at precise distances from the generator orifice. Thus, depending on where the PDPA probe was located, the drop was either a prolate spheroid, sphere or oblate spheroid. An imaging system was used to measure the aspect ratio. In addition, a simple analysis was performed to predict the measurement error. In this case, the radii of curvature of ellipsoidal drops with equal volume were calculated. Figure 9 shows the response of the phase Doppler method at different aspect ratios. The results of the analysis are shown with the experimental results. Note that the lowest two experimental points that deviate from the

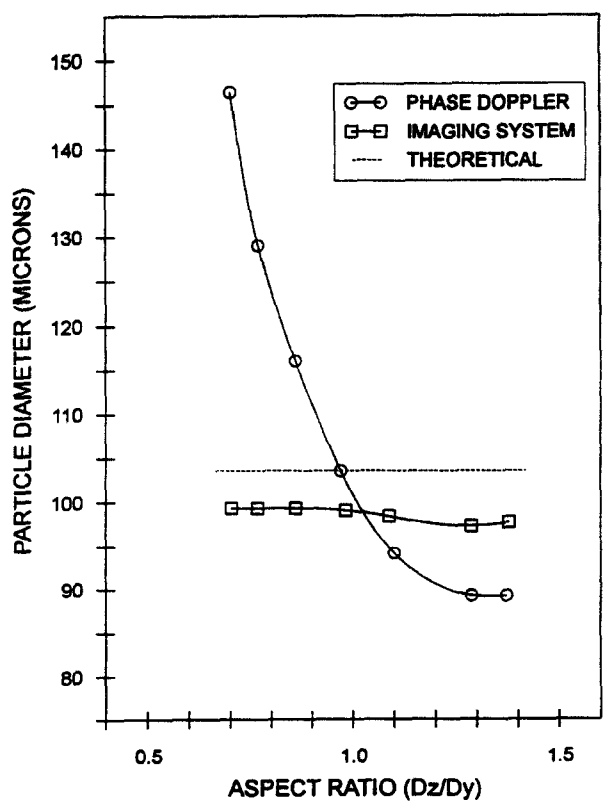


Figure 9. Response of the phase Doppler method to deformed particles with different aspect ratios.

theoretical curve must be in error. It is not possible to have an increase in the aspect ratio (major to minor axis lengths) without a local change in the radius of curvature. Note that for aspect ratios of between 0.75 and 1.25, the error is approximately symmetric, so if the drop was oscillating randomly, the average size would be measured to be very close to the actual size.

*Measurement of Non-spherical Particles: the Ratiometric Method*

In order to obtain simultaneous size and velocity measurements of irregularly-shaped particles, light scatter detection at confocal forward scatter or small off-axis angles is necessary. The validity of this approach has been demonstrated by Jones (1988), Gebhart & Anselm (1988), Killinger & Zerrull (1987) and others. At small off-axis angles the light scattering by particles greater than the wavelength may be described by Fraunhofer diffraction, which treats the particle as an opaque disk. The angular distribution of the scattered light is inversely proportional to the dimension of the particle. If the light scatter detection is symmetric about the transmitted beam, the measured average size tends to be equal to the equivalent spherical diameter, since the particles pass the beam at random orientations. This is true if the aspect ratio of the particle is not too large. For smaller particles, the distribution of the scattered light tends to be less dependent upon the shape, see Killinger & Zerrull (1988).

Efforts by Maeda *et al.* (1986), and by Gouesbet *et al.* (1988) were made in an attempt to use the light scattering intensity detection method combined with the LDV to measure the size and velocity of both spherical and nonspherical particles. A key problem with the approach was the unknown incident light intensity on the particle due to the random trajectories through the beam. In their approach, the Gaussian laser beam intensity profile was modified to form a nearly "top hat" intensity profile. This method was marginally successful but suffered from the problem of particles passing the edge of the beam being registered as smaller particles. Another approach, first offered by Bachalo (1979), was to use a pair of coaxial beams of different polarization or wavelength to resolve the ambiguity in the incident light intensity associated with the random particle trajectories through the Gaussian beam profile. A more recent approach has been proposed by Bachalo (1989) to overcome many of the shortcomings identified in the previous approaches.

The ratiometric method combines the LDV method with the measurement of the scattered light intensity to infer the particle size. As such, near forward scatter light can be used for measuring irregular-shaped quasi-spheres and off-axis detection can be used when measuring spheres. A key feature of the method is that a relatively straightforward and practical means is used to remove the incident intensity ambiguity due to the Gaussian beam. Basically, as first proposed by Bachalo (1979), the ratiometric technique for particle characterization consists of a laser beam which is split into two beams having approximately equal intensities. One of the beams is passed through a beam expander while the second one is directed to a polarization rotator. Subsequently the two beams are focused to a common point. Particles passing through the probe volume scatter light which is collected by the receiver lens and focused onto photodetectors which are coupled to a signal amplitude detection device for further analysis and data reduction (figure 10). The approach employs a beam ratio of approx. 3:1. The two coaxial laser beams which are focused into a common point, establish two confocal beam diameters, as is shown in figure 11. The particles that

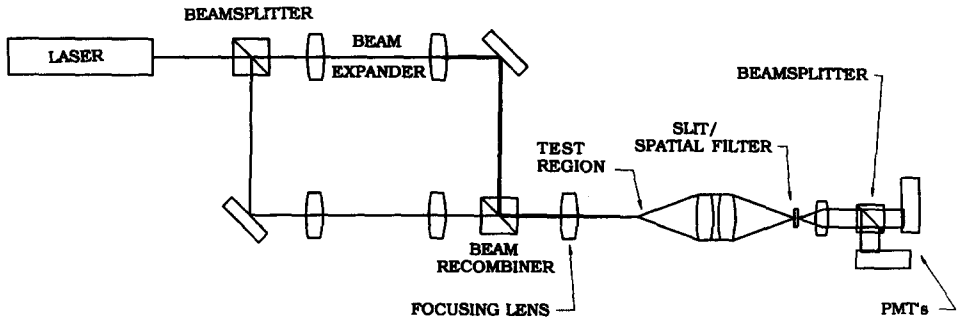


Figure 10. Optical configuration of the ratiometric particle analyzer.

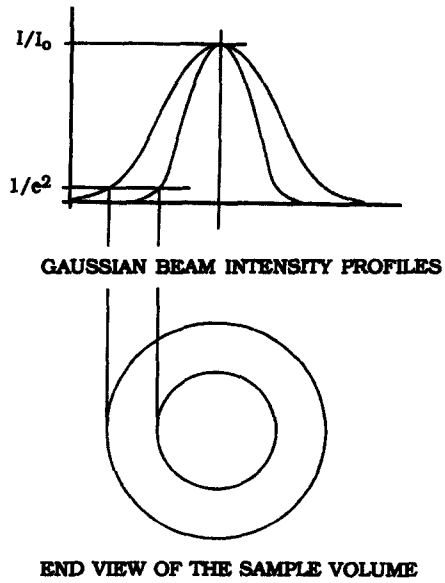


Figure 11. Two confocal beam diameters for trajectory determination.

pass through the focused beams will scatter light with an intensity that is a function of their diameter, index of refraction and intensity of the incident light, which depends on the trajectory of the particles through the beams.

With the approach, a particle passing on an arbitrary path through the probe volume, produces a signal from detectors 1 and 2. In order to determine the incident intensity on the particle, the trajectory defined by the distance $x_p$ from the center of the beam must be known. The Gaussian intensity distribution of the incident beams is given by

$$I_\xi = I_{0,\xi} \exp(-2x_\xi^2/b_\xi^2)$$

where the subscript $\xi$ refers to either beams 1 or 2, $I_0$ is the peak intensity of the beam which may be measured, $x$ is the radial coordinate of the beam and $b$ is defined, by convention, as the radius wherein the intensity $I$ is equal to $1/e^2$ of the peak intensity, $I_0$. The radius $b$ can be measured also for each beam.

The energy scattered by particles crossing beams 1 and 2 can be specified as a function of the scattering parameters $Q_1$ and $Q_2$. Parameters $Q_1$ and $Q_2$ can be computed if the characteristics of the particles, such as shape and material, are known or can be determined by previous calibration with samples which have known sizes. The scattering coefficients depend on the diameter, index of refraction and shape of the particles, wavelength and polarization of the incident light and angle of collection. These coefficients are generally calculated or obtained by calibration as a function of the size of the particle and subsequently integrated into a look-up table, such that if $Q$ can be determined, a diameter $d$ can be read off the table. $Q(d)$ will, therefore, be specified as a function of $d$.

For an arbitrary particle path $x_p$, measured from the center of the beams and shown schematically on figure 12, the scattered peak intensities may be expressed as,

$$I_{sc,1} = I_{01} Q_1(d) \exp(-2x_p^2/b_1^2)$$

and

$$I_{sc,2} = I_{02} Q_2(d) \exp(-2x_p^2/b_2^2)$$

Taking the ratio of the two equations yields,

$$\frac{I_{sc,1}}{I_{sc,2}} = \frac{I_{01} Q_1(d)}{I_{02} Q_2(d)} \exp(-2x_p^2(1/b_1^2 - 1/b_2^2))$$

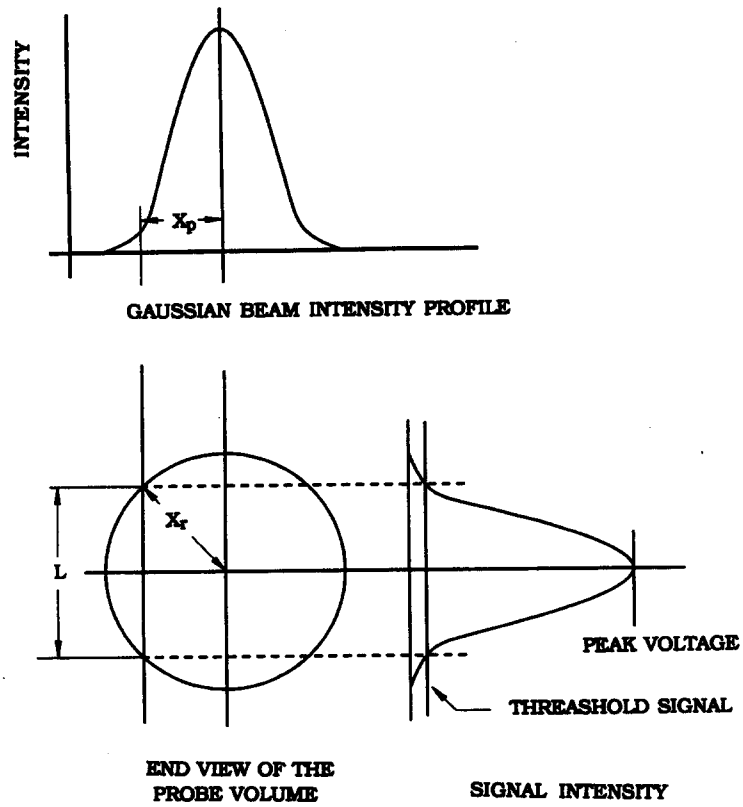


Figure 12. Arbitrary particle path through the Gaussian beam probe volume.

Solving for $x_p$ results in the following expression,

$$x_p = \left\{ \frac{1}{2} \left( \frac{b_1^2 b_2^2}{b_1^2 - b_2^2} \right) \log \left[ \frac{I_{sc,1}}{I_{sc,2}} \frac{I_{02}}{I_{01}} \frac{Q_2(d)}{Q_1(d)} \right] \right\}^{1/2}$$

The ratio $Q_2(d)/Q_1(d)$ is determined by calculating the light scattering of a spherical particle for the respective polarizations, which is the only parameter that is different between the two quantities. When beams of different wavelength are used, the scattered intensities by a particle in the probe volume are proportional, to a first approximation, to the square of the diameter of the particle. Preliminary computer modeling has shown that the ratio of the scattering coefficients remain constant over the particle size range of interest if the incident polarization of the two different laser wavelengths is the same; that is, to a first approximation $Q_2/Q_1$ is not a function of $d$. The ratio of the scattering coefficients is expected to change with a different set of physical parameters, and has to be calculated and incorporated into the look-up tables.

The incident beam intensities, $I_{01}$ and $I_{02}$, are determined *a priori* by calibration of the system. Measurements of $I_{sc,1}$ and $I_{sc,2}$ are obtained for each particle based on the signal amplitude measurements. Thus, the $x_p$ are calculated explicitly from the measured quantities for each particle size and trajectory. With $x_p$ determined, the equations may be rearranged as

$$Q_1(d) = \frac{I_{sc,1}}{I_{01}} \exp(2x_p^2/b_1^2)$$

and

$$Q_2(d) = \frac{I_{sc,2}}{I_{02}} \exp(2x_p^2/b_2^2)$$

to obtain $Q_1(d)$ and $Q_2(d)$. The values of $Q_1(d)$ and $Q_2(d)$ are subsequently used with the respective look-up tables to obtain the values of the diameter of the particles. Even in those cases when the Lorenz–Mie theory is used to generate the scattering parameters, calibration is still

required to determine the constants that describe the collection efficiencies and gains of the system. The Lorenz–Mie theory must be used with some reservation since the theory does not apply to non-spherical particles. With certain light scatter detection geometries, the theory will offer a good approximation.

For irregular-shaped particles the light transmission through the particle will not be the same as for spherical particles. Therefore, oscillations in the response curves (i.e. scattering coefficients) which arise from the interference between the refractive and diffractive light scattering will be significantly dampened.

The method is currently being implemented into a commercial instrument to address the need for a method that can measure the size and velocity of irregular-shaped particles. Preliminary tests of the method showed good resolution and accuracy.

*Flow visualization*

A novel flow visualization system showing the interaction of particles with the large scale eddies formed in a shear layer has been described by Hancock *et al.* (1992). The method involves the use of a $TiCl_4$-laden gaseous flow environment in which water drops are injected. The water drops react rapidly with the $TiCl_4$ to form a large number of $TiO_2$ particles that are on the order of 1 $\mu$m in diameter. These particles trace the path of the flow passing the water drops. A laser light sheet or other suitable illumination is used to scatter light from the drops and from the $TiO_2$ particles used to visualize the flow. Figure 13 shows an example of the visualization that is possible with this method. The figure shows a 70 $\mu$m water drop interacting with the vortices produced by the shear layer. The figure on the left shows a continuous stream of drops, whereas the figure on the right shows a single drop with the vapor line or stream of $TiO_2$ particles tracing the vaporline. This example shows how particle clusters may form as a result of the interaction with large scale eddies. It is easy to anticipate from the visualization how, in a polydispersion, particles of different sizes will respond to the eddies. This method may be expanded to study drops over a range of sizes to characterize the particle response to large scale eddies.

*Particle imaging methods*

Particle imaging methods are sometimes used to collect instantaneous particle size, shape, local concentration and spatial distribution information over a finite region of interest. The

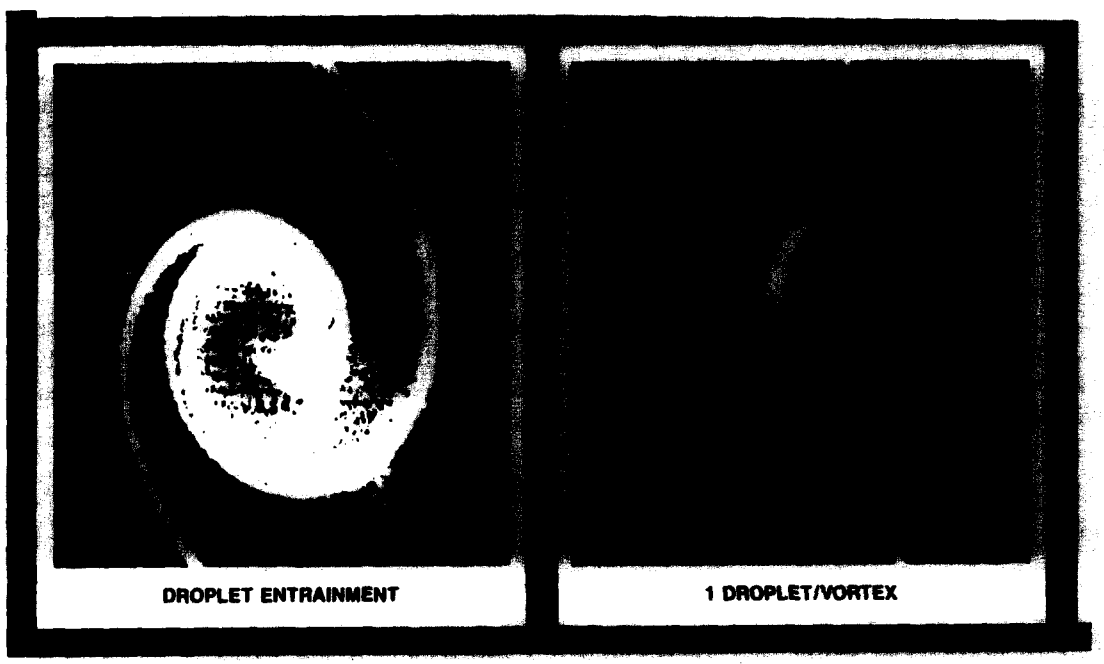


Figure 13. Water drop interaction with a large scale eddy using $TiO_2$ for the flow visualization (from Hancock *et al.* 1992).

instantaneous velocity field can also be captured by analysis of multiple exposure images using the particle image velocimetry (PIV) technique which is discussed in the next section. The advantage of these techniques over other alternatives is that they produce detailed spatial distribution information for an instant of time. The major drawback is that they often require time intensive analysis which often limits the amount of data which can be collected and processed.

A variety of means are available for recording images of the particles in the flow. These include conventional film photography, holographic recordings, or direct electronic imaging using CCD or CID area detectors. In all cases it is important to limit the duration of the exposure so that the motion of the particles does not cause excessive unwanted blurring of the particle images. This is commonly achieved by using a pulsed laser (typically either a frequency doubled Nd:YAG or a ruby laser) which can deliver a very bright illumination pulse lasting on the order of $10^{-8}$ s. Even relatively small particles traveling at supersonic speeds can be clearly imaged with such short exposure times. At low speeds, or for large particles, other light sources with longer exposure times and/or less flash energy may be used.

For both conventional film photography and electronic imaging it is extremely important that the particle images are in focus. Particles which are out of focus will produce a blurred image which makes the particle appear larger and perhaps more spherical than it is in reality. The measured location of these particles will also be in error as the magnification ratio of the optics system is a function of the distance from the lens to the particle. Decreasing the aperture of the lens system can be used to increase the depth of field, but this improvement comes at the expense of reduced illumination to the image plane. In order to confine the measurements to those particles which will be in a single plane at the correct focus distance, optics are usually employed to form a sheet of illumination. In high particle density environments, scattering by particles will both attenuate the intensity of the remaining portion of the sheet and will also increase the background illumination level. Both effects tend to reduce the signal-to-noise ratio of the resulting image, but typically the analysis can still be limited to those particles which are within the light sheet. In addition, particles located between the light sheet and the camera lens can attenuate the scattered light and obscure the image.

To circumvent the depth of focus limitations of conventional and electronic photographic techniques, holographic recording of the three-dimensional structure of the multiphase flow have been used (Thompson 1967, 1982; Nyga *et al.* 1990). After the holographic plate is chemically processed, the three-dimensional image must be reconstructed using a coherent illumination source. The reconstructed three-dimensional scene can then be inspected using a CCD camera. The focus plane can be traversed through the stationary scene to record multiple images of each particle. The location of the particle must be deduced by determining which interrogation image has captured that particle in the best focus. Analysis is further complicated by speckle noise (a by-product of the coherent illumination), and by variation in magnification ratio as a function of particle position. The difficulty associated with obtaining and chemically processing the holograms, and the complexity and time intensive nature of the subsequent analysis have probably been the major factors in limiting the widespread use of this technique.

All of the imaging techniques must contend with the light scattering properties of the particles. The perceived shape and size of the particles can be strongly influenced by the scattering mechanisms present. This is especially true when using highly directional coherent illumination and limited aperture imaging lenses. For instance, reflection will be the dominant light scattering mode from spherical water droplets illuminated with a sheet of light and imaged with a camera pointed normal to this sheet. However, only a small portion of the surface of the droplet will reflect light into the limited aperture of the camera lens. The size of this region will increase as the aperture of the camera lens increases. The perceived size of the droplet will thus be less than the actual size, and will be dependent on the camera aperture. It may be possible to account for this effect with intelligent analysis of the image, but further complications, such as random orientations of non-spherical shapes, may limit the ability of the analysis to account for light scattering effects.

In order to obtain sufficient resolution, particle imaging methods typically have required that the field of view be limited such that the images of the smallest particles span at least 5–10 pixels in each direction. For a commercial grade CCD video camera with a resolution

of nominally 500 × 700 pixels, this would limit the field of view to about 50–100 times the diameter of the smallest particle of interest, depending on the particle sizing resolution required. Thus, a flow with particles in the 50–500 $\mu$m diameter range might limit the field of view to just 5 × 7 mm. A scientific grade 2048 × 2048 pixel camera would increase the field of view to 20 × 20 mm at the same resolution. Film can provide equivalent resolution over an even larger field of view, but it must be chemically processed and then digitized prior to analysis. To increase the field of view of a CCD-based imaging system, a method of particle sizing by pixel intensity measurement has been partially developed and tested by Hofeldt (1991), but this exhibited substantial sizing errors resulting from difficulties in determining the incident intensity which is a function of the particle position in the direction normal to the light sheet.

*PIV for multiphase flows*

The displacement of particle images over a known time interval can be used to determine the particle velocity. This family of techniques is commonly referred to as particle image velocimetry (PIV), although a number of other terms are often used to describe various subsets of the wide range of similar techniques (Adrian 1991). To obtain reliable velocity information the time between exposures must be selected so as to obtain a sufficient displacement to achieve an acceptable velocity resolution, but must not be so large that the particle moves out of the field of view or out of the plane of illumination. The local velocity is then estimated from

$$\mathbf{u} = \frac{\Delta \mathbf{x}(\mathbf{x}, t)}{\Delta t}$$

With the PIV system, shown schematically in figure 14, the particles in the fluid are illuminated with a sheet of light, normally provided by a pulsed laser although other sources may also be used. The particles scatter light to an imaging device. The particle images may be recorded photographically on film, or electronically using a CCD or CID camera. Film has the advantage that it provides very high resolution over a large area. Recent advancements in CCD technology have pushed the resolution limits to beyond the 25 million pixels per image mark. The use of high resolution CCD and CID cameras eliminate the need for both the chemical processing of the film, and the subsequent digitization of the image. As an alternative to two-dimensional recording with film or CCDs, holographic recordings have been used to obtain three components of velocity information

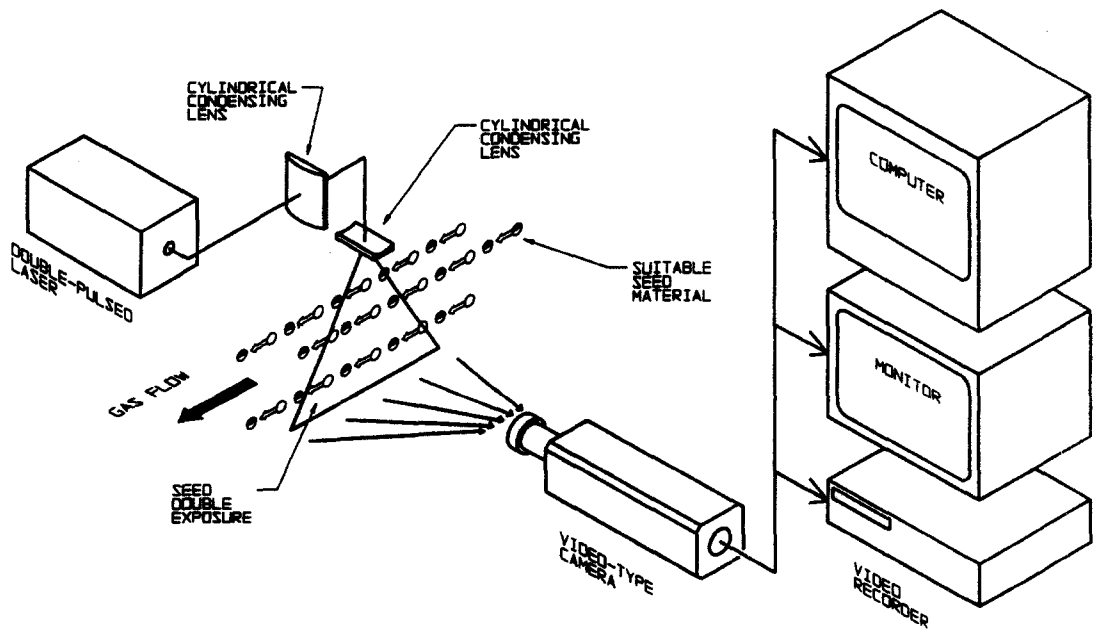


Figure 14. PIV system using CCD camera technology.

over an entire volume of the flow (see Hinsch 1993; Bernal & Scherer 1993; Thompson 1989).

A variety of techniques have been used for analysis of the images. For low particle density flows a particle tracking technique is typically employed. Individual particles are identified, their centroids are located, and the matching particle image(s) created by additional exposures are similarly identified and located. The distance between particle pairs is then used to calculate the velocity. As the particle density increases, it becomes more and more difficult to accurately determine which particle images correspond to pairs of exposures of the same particle, and which are simply neighboring particles. Statistical means are used to determine the mean offset of the pairs of particle images within a subset region of the photograph. In early implementations of PIV, this was accomplished optically using the Young's fringes method. This method requires that a coherent laser beam be used to illuminate the double exposure image. The correlation between the double exposure particle images causes a diffraction pattern to form. The fringe spacing and orientation of this pattern is recorded with a CCD camera and measured to determine the local velocity and direction. With advances in computational speed, and the development of efficient auto-correlation algorithms, many researchers have come to the opinion that direct statistical analysis of a digitized image is simpler and more reliable than the Young's fringes process (Adrian & Yao 1984; Adrian 1988).

All of these methods result in a velocity orientation and magnitude in the plane of interest, but the direction or sign of the velocity vector is often not known. This occurs whenever the first exposure cannot be distinguished from the second. This is similar to the velocity direction ambiguity which occurs in LDV. In LDV this ambiguity is eliminated by imposing a frequency shift on one of the two laser beams so that the fringes move in the direction opposite to the assumed flow direction. Stationary particles will produce a Doppler signal with the shift frequency, while particles moving in the direction of the fringe motion will create a lower frequency, and particles moving in the opposite direction will create a higher frequency. Similarly, in PIV an image shift is often imposed in which the second image of a stationary particle will be offset a preset amount from the first image. The image of particles moving in the direction of the shift will be offset further, particles moving in the other direction will be offset less. Alternative methods for resolving the directional ambiguity are based on identifying the order in which the particles' images were created. One implementation uses color coding of the particle images by using a different color for each of the two laser pulses and recording the results on color film (Smallwood 1992).

To date, the vast majority of the applications of PIV have been in experiments concentrating on single-phase flow. In these experiments seed particles are added to the continuous phase. Ideally, the size of these particles is tightly controlled and is selected to insure that they are small enough to follow the flow. The concentration of the particles can also be adjusted to control the image quality. In multiphase flows, the particle size and density are set by the application. This reduces the freedom of the experimentalist in controlling many of the parameters which affect the data analysis routines.

*Particle temperature measurement or discrimination*

In many multiphase flow applications, the mixing of two different types of particles carried within the continuous phase may be of interest. It may also be of interest to determine the temperature of the spherical transparent particles. This information can be obtained by measuring the location of the rainbow angle relative to the incident laser beam (Roth *et al.* 1993; Sankar *et al.* 1993). The rainbow angle which manifests as a peak in the light scattering intensity depends upon the drop or particle index of refraction. The *in situ* measurement of the index of refraction can then be related to the particle temperature or in the mixing studies, it can be used to identify particles of one material relative to another in the flow to identify and separate the size and velocity measurements from each type of particle.

The occurrence of rainbows can be understood with the help of the simple geometrical optics based theory proposed by Descartes several hundred years ago. Using geometrical optics assumptions, the scattering of light by spherical particles can be described as a combination of diffraction, external reflection, refraction and refraction occurring after multiple internal reflections. Furthermore, adopting van de Hulst's notation (1981), $p = 0$ refers to externally reflected

light, $p = 1$ refers to refracted rays, $p = 2$ refers to rays that emerge from the droplet after undergoing one internal reflection, and so on. For each scattered ray, the scattering angle bears a definite relationship to the incident angle. The location of the primary rainbow can then be understood to correspond to that scattering angle at which the angular relationship for $p = 2$ goes through an extremum.

At the rainbow angle, the scattered intensity achieves a local maximum as seen from the convergence of light rays. To one side of the rainbow angle is a shadow region into which no rays emerge and to the other side is a lit region. Similarly, the secondary rainbow corresponds to the scattering angle extremum for $p = 3$ rays. For example, for water droplets, the primary and the secondary rainbows occur at scattering angles of 137.9 and 128.8°, respectively. The dark region between the primary and the secondary rainbow is historically known as Alexander's dark band. Rainbows of order greater than $p = 3$ can also be present, but in general, are very weak in intensity.

Rainbow refractometry takes advantage of the fact that the rainbow angle is a function of the refractive index of the droplet. Therefore, by measuring the rainbow location with the help of a linear array detector such as a CCD, the refractive index of the droplet can be determined. Since refractive index varies with temperature, the droplet temperature can also be inferred if the relationship between the refractive index and temperature is known *a priori*. The rainbow angle also exhibits a dependence on the droplet size, especially for droplets less than about 100 $\mu$m in diameter, and therefore a knowledge of the droplet size is also required for accurate measurement of the droplet temperature in spray flames. Fortunately, by integrating the rainbow thermometric technique with an independent particle sizing technique, the droplet temperatures can be accurately measured.

The well-established and widely accepted phase Doppler interferometric technique for measuring spherical particle size and velocity in complex sprays was a natural choice for integration with the rainbow thermometry. There was an added advantage to this integration since the particle size measurement with the phase Doppler technique is also dependent on the refractive index of the droplets. When the instrument has been configured such that the scattering is dominated primarily by refracted rays of order $p = 1$, the dependence on refractive index is not large. For example, theoretical phase Doppler response studies show that for a 200°C change in kerosene temperature, the sizing error is about 8%. Furthermore, this uncertainty can be reduced to about 4% if a refractive index value is selected that corresponds to a temperature that is half way between room temperature and the boiling point. In applications where the refractive index varies more drastically or greater accuracy is required, an iterative technique can be used to simultaneously obtain the true droplet temperature (refractive index) and droplet size. Finally, it is important to recognize that the theoretical phase Doppler response studies that were undertaken assume that the droplets have a uniform refractive index. A study has recently been conducted by Schneider *et al.* (1993) to determine the magnitude of sizing errors as a result of internal refractive index gradients within droplets.

In summary, the implementation of rainbow thermometry for droplet temperature measurement requires two functional relationships; a relationship describing the dependence of the rainbow angle on the droplet refractive index and size, and another describing the dependence of the refractive index on temperature for the desired liquid. The former can be computed using the exact Lorenz–Mie theory. The latter can either be obtained from reference handbooks or can be calibrated in the laboratory. In the study of different dispersed materials that have different indices of refraction, it is easily possible to use the method to assess the mixing characteristics of the dispersed phase.

*Methods for studying turbulent mixing of the dispersed phase*

The turbulent mixing of two fluids, a fluid and a dispersed phase, or two dispersed materials in a fluid are of interest in the research on multiphase flows. Such mixing studies can be carried out using the phase Doppler method integrated with the rainbow method as described in the preceding section. If the dispersed phase particles have a size range that is from a few microns to 100 microns, it is not always possible to separate the dispersed phase velocity measurements from the fluid flow based on particle size. This is true because larger seed particles may be required if both the dispersed

phase and fluid phase velocities are to be measured at the same time. An easier less expensive approach may be used in many such cases (Sankar *et al.* 1990). In this approach, the seed particles or dispersed phase particles are tagged with a fluorescent dye such as fluorescein disodium salt or rhodamine B dissolved in water. These dyes absorb light at wavelengths of around 500 nm and fluoresce at wavelengths centered around 560 nm. The basic studies showed that the dye concentration in the particles cannot be too high, otherwise a severe loss in the Doppler signal-to-noise ratio will occur. This is due to the fact that the fluorescent light is not coherent so it does not provide information on the Doppler difference frequency or signal phase. The Doppler signal requires that some of the incident light is scattered elastically by the particle. Proper selection of the dye concentration through experimentation produced both good fluorescent and scattered signals simultaneously.

Implementation of the method required the incorporation of a second receiver unit to the standard phase Doppler instrument. The fluorescence receiver was outfitted with a line filter that only admitted the light at the fluorescence wavelength. The detection of dye-tagged particles was immediately communicated to the phase Doppler instrument. The instrument then sorted the particle measurements into dye-tagged and standard particles. Such discrimination of the particles could then be used to determine the relative concentrations of the dispersed phase particles at points in the fluid.

*Particle drag coefficient determination*

A critical parameter in any study of the reaction of particles in a fluid is the drag coefficient, $C_D$. Accurate knowledge of the particle drag coefficient in both highly turbulent and high particle number density environments is an important element in the development of more reliable models for two-phase turbulent flows. A number of correlations for $C_D$ have been developed (Torobin & Gauvin 1960; Brown & Hutchinson 1979), primarily measuring the terminal velocity of non-deformable isolated spheres falling in a quiescent environment. Questions remained as to the effect of particles in the neighborhood and the effect of the flow stream turbulence. A number of recent theoretical studies have addressed these problems, for example, Sirignano (1993).

Experiments were designed to assess the effects, if any, of the presence of neighboring particles and fluid turbulence on the particle drag (Rudoff *et al.* 1991). In these experiments, a stagnation flow was generated with a right circular cylinder mounted in the test section of a wind tunnel. The stagnation streamline produced by the cylinder created well-defined flow deceleration. Flow speeds of 15 and 29 m/s were used. Spray nozzles were mounted 1.14 m upstream of the cylinder. These pressure atomizer type nozzles created polydispersions of water drops. The number densities were 300 $cm^3$ and 700 $cm^3$ for the higher concentration case. In addition, the turbulence intensity of the wind tunnel was increased from its normal value of approx. 2–7% with the use of a grid. The phase Doppler instrument was used to simultaneously measure the drop size and velocity. The deceleration between the measurement points, along with the gas and drop size and velocity were used to calculate the droplet drag and the Reynolds number for each drop size class. The drops 3 $\mu$m and smaller were used to define the gas phase velocity. Data were collected along the stagnation streamline from 330 mm upstream to within 7 mm of the front surface of the cylinder. The drag coefficient was determined for discrete particle size classes.

The momentum equation was used to determine the expression for the drop drag coefficient as

$$C_D = \frac{2m_p \rho_p}{U_r^2 A_p \rho} u_p \frac{du_p}{dx}$$

where $\rho_p$ is the particle density, $U_r$ is the relative velocity between the particle and the air, $A_p$ is the frontal area of the particle and $u_p$ is the particle velocity. The calculated $C_D$ values were compared to the empirically derived curve fit for the values for a spherical particle given by Torobin and Gauvin.

The phase Doppler instrument was used to measure the particle size and velocity at a number of axial stations. An example of the mean axial velocities for the discrete size classes is shown in figure 15, plotted with respect to the distance from the cylinder. The potential flow velocity is also shown on this figure. The results were used to estimate the drag coefficient, and an example of these results is shown in figure 16. It is interesting to note that the correlation of Torobin and

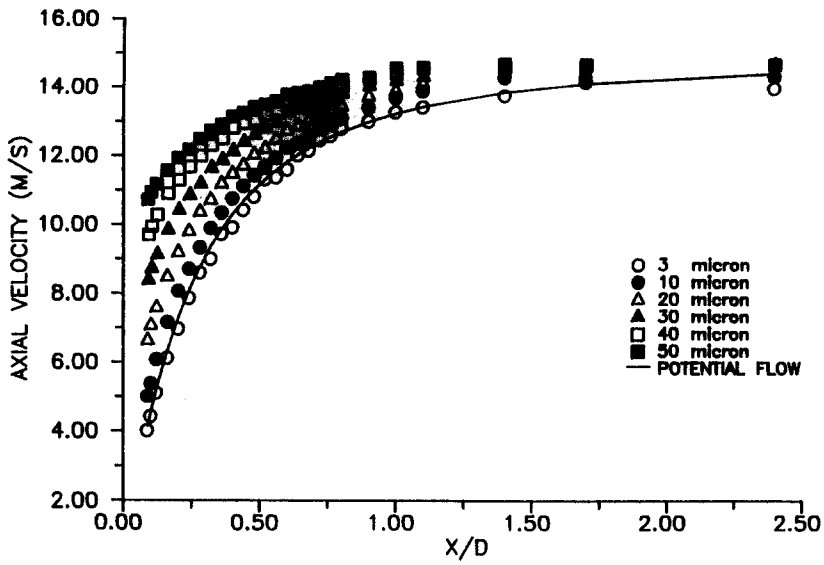


Figure 15. Mean axial velocity for discrete size classes of particles approaching a cyclinder on the stagnation streamline, low turbulence, high number density.

Gauvin fits the data reasonably well, even for the case of high turbulence and with deformable drops.

An estimate of the drop deformation stated earlier can be obtained for the worst case of the largest drops near the cylinder where the relative velocity was the greatest. The deformation of the drop can be estimated from Hinze (1947) as

$$\left(\frac{2\delta}{d}\right)_{\max} = -0.095\rho \frac{d}{2}\frac{U_r^2}{\sigma}$$

where $\delta$ is the radial displacement of the droplet surface from its position in the undeformed state, $\rho$ is the density of the air or surrounding fluid, $U_r$ is the relative velocity between the fluid and the drop, and $\sigma$ is the drop surface tension. This deformation is not especially large so it is not surprising that the drag correlations agreed with those of a solid sphere. Future work is needed

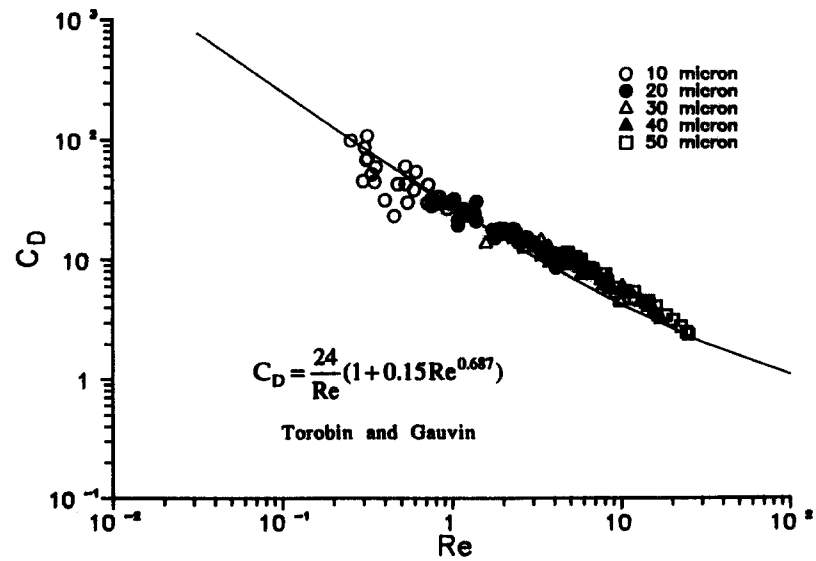


Figure 16. Drag coefficient vs Reynolds number for discrete size classes, derived from the low turbulence, high number density case, compared with the correlation of Torobin & Gauvin.

to address higher levels of free-stream turbulence, larger drops and larger drop Reynolds numbers. This will allow a better determination of the drop–drop interactions and the effects of turbulence and deformation on the drop drag.

*Turbulent dispersion of particles*

Basic experimental studies of the particle response to turbulent flows are important to the understanding of how the various flow and particle parameters affect the particle dispersion. Of interest is the degree to which particles of various size classes will respond to the turbulence fluctuations and will be entrained by the interaction with the vortices. Accumulation of the smaller particles into the vortices can lead to drop clusters or local high drop concentrations and segregation of the smaller drops from the large drops, as well as the dispersion of the particles. The interaction of the particles with the various turbulence length scales will also create voids or regions of low concentration, at least for certain size classes.

Relationships are given for reference that reveal the parameters affecting the particle response to the flow velocity fluctuations and; hence, to the drop dispersion. Numerous studies have been conducted in an effort to define the behavior and response of particles in a turbulent flow, including Hinze (1972), Brown & Hutchinson (1979), Simo & Lienhard (1991) and Hardalupas *et al.* (1992). The characteristic particle response time derived from the Stokes' law relaxation time (time required for the injected particle's velocity to drop by a factor of $1/e$) is given, following the fundamental analysis of Hinze, as

$$\tau = \frac{4 d_p \rho_p}{3 C_D \rho U_r}$$

which, for a Stokes flow drag law correlation, may be expressed as

$$\tau = \frac{d_p^2}{12\nu} \frac{(2\rho_p + \rho)}{3\rho}$$

where $d_p$ is the particle diameter, $\nu$ is the kinematic viscosity, $\rho_p$ is the particle density, $U_r$ is the relative velocity between the particle and the air flow and $\rho$ the fluid density. The above expression holds for a particle Reynolds number, $\mathrm{Re}_p = \rho d_p U_r / m \ll 1$. If this condition is not satisfied, then a non-linear drag law such as that of Torobin & Gauvin (1960) must be used:

$$C_D = \frac{24}{\mathrm{Re}_p} [1.0 + \tfrac{1}{6} \mathrm{Re}_p^{0.66}]$$

The Stokes flow drag coefficient and the above value are within a factor of 3 of each other for Reynolds numbers as high as 50. With the further assumption that the ratio of fluid-to-particle density is small ($\rho/\rho_p < 10^{-3}$) which is true in the present case, the expression simplifies to

$$\tau = \frac{d_p^2 \rho_p}{18 \nu \rho}$$

which indicates that the characteristic particle response is proportional to its diameter squared.

The particle response to the large turbulent scales is most relevant to the dispersion of the particles in the flow since it is the large scales that are the most effective transport mechanism. Referring to the analysis of Hinze yields an expression that approximates the response as

$$\frac{d_p}{\Lambda} \leqslant \left[ \frac{u' \Lambda}{\nu} \left( \frac{\rho_p}{\rho} + \beta \right) \right]^{-1/2}$$

where $\Lambda$ is the macroscale of the turbulence, $u'$ is the rms velocity of the gas phase and $\beta$ is given by

$$\beta = 1 + \frac{\rho}{2\rho_p}$$

which is approx. equal 1 for the present case. The macroscale of turbulence may be taken as equal to the cylinder diameter, $D$. The above expression can then be simplified to

$$\frac{d_p}{D} \leqslant \left[ \frac{u' D}{\nu} \left( \frac{\rho_p}{\rho} + 1 \right) \right]^{-1/2}$$

Thus, only particles of density $\rho_p$ that are smaller than $d_p$ given in the above expression will respond to turbulence with rms fluctuations of $u'$. This may also be stated in terms of Stokes number (Humphries & Vincent 1978), as

$$St_r = \frac{T_t}{\tau}$$

where $T_t$ is the characteristic time scale of the large scale eddies given as

$$T_t = \frac{D}{U_{re}}$$

where $U_{re}$ is the relative velocity between the particle and the eddy convection velocity. A simple substitution results in the expression for the particle transit Stokes number as

$$St_r = \frac{1}{\tau}\frac{D}{U_{re}}$$

which must be much greater than 1 for the particle to respond to the turbulent eddy. That is, the interaction time with the eddy must be longer than the characteristic response time of the particle.

Centrifugal forces will also influence the dispersion of the spray drops. Small particles will follow the rotation of the eddy or vortex, whereas progressively larger drops will cross streamlines and be centrifuged out of the eddy (Hardalupas *et al.* 1992). The magnitude of the centripetal forces relative to the Stokes drag forces are estimated using the centrifuge Stokes number (Dring & Suo 1978) as

$$St_\psi = \frac{18\nu}{\psi d_p^2}\frac{\rho}{\rho_p}$$

where $\psi$ is the angular velocity.

*Axisymmetric jet*

Measurements of the jet velocity profile were obtained at an axial location of $x/D = 30$ and a jet Reynolds number of 50,000. Figure 17 shows the mean radial distribution of the axial velocity, $U$, along with the well-known correlation for the jet. These data show that the jet flow field is in close agreement with the expected result. Figure 18 provides similar information for the axial turbulence intensity. Simultaneous measurements of the particle size and velocity allowed the determination of the response of the various particle classes to the fluid turbulence.

Figure 19 provides an example of the particle response data that is available. In this plot, each dot on the graph represents an individual measurement of each particle's size and velocity. Note

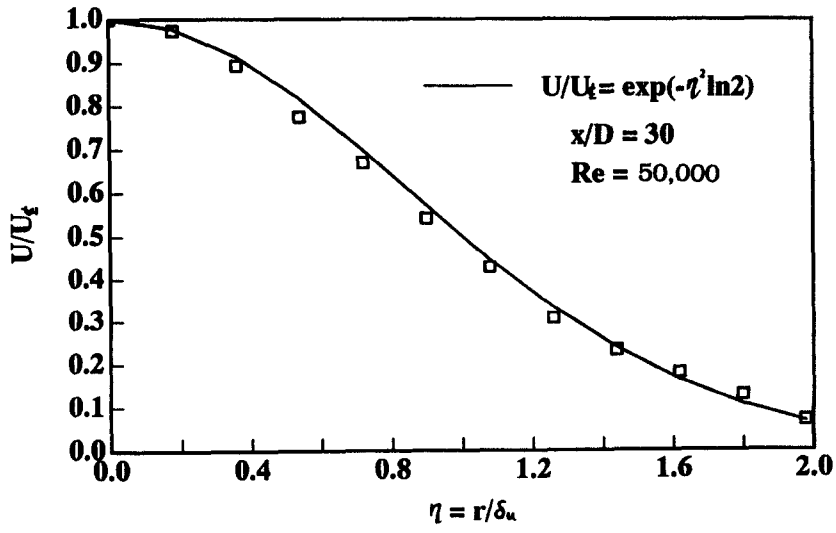


Figure 17. Radial variation of the mean axial velocity component.

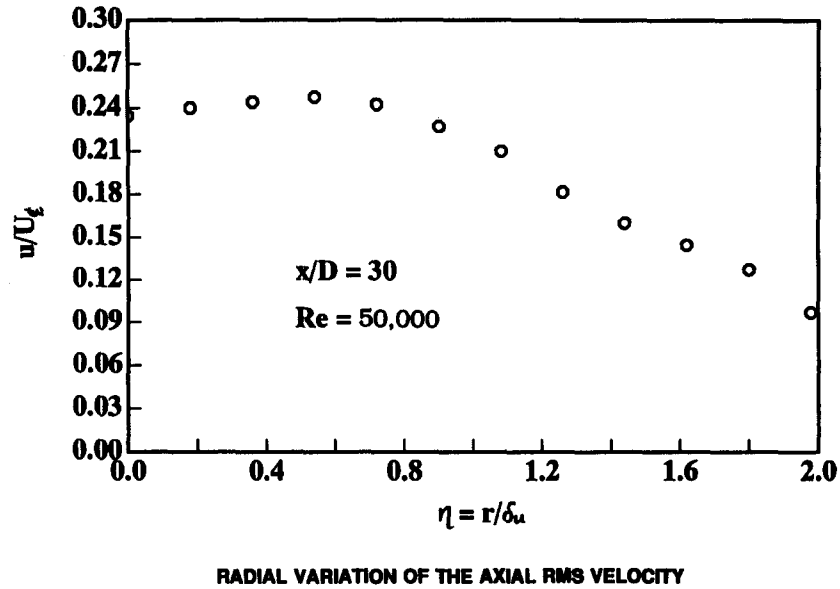


Figure 18. Radial variation of the turbulence intensity for the axial velocity component.

that for this case, particles with diameters below approx. 3 $\mu$m respond to the turbulence fluctuations, as noted from the range in the velocity excursions in comparison to the 1 $\mu$m particles. The spread in the velocity distribution (essentially proportional to the rms velocity) decreases noticeably with an increase in the particle diameter. The plot of the rms velocities for the range of particle diameters is given in figure 20 for the axial, $U$, and radial, $V$, velocities. The point to note is that particles as large as 5 $\mu$m were able to respond to the velocity fluctuations in the axial direction. However, in the radial direction, only particles as small as 1 $\mu$m respond to the turbulence fluctuations. This information was used to conclude that the turbulence induced flow accelerations were much larger in the transverse direction. In fact, the particle lag for the different size classes may be used to estimate these flow accelerations.

*Cylinder flow wake field*

Particle response to large scale eddies is a fundamental mechanism in the particle dispersion and cluster formation. To investigate these phenomena, the interaction of a spray with a cylinder wake was considered. This flow field provided a periodic shedding of vortices which entrained the particles and carried them downstream. The flow shedding was a reasonable simulation of the eddy formation in turbulent flows. Since the particle field was relatively dilute, the so-called one-way

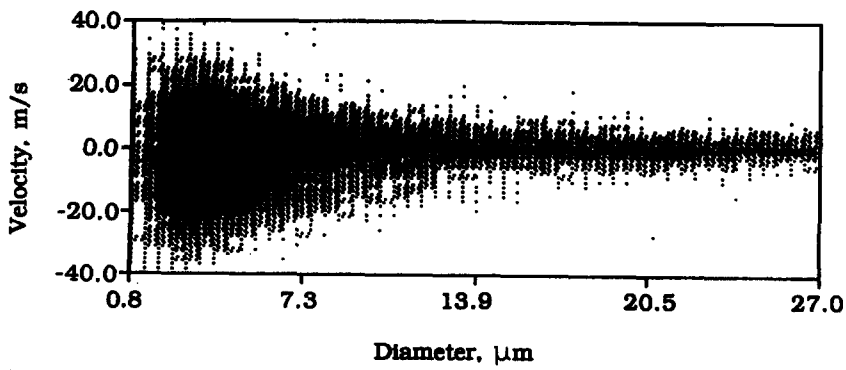


Figure 19. Size velocity correlations for the radial velocity component. Each point on the figure represents a single particle measurement.

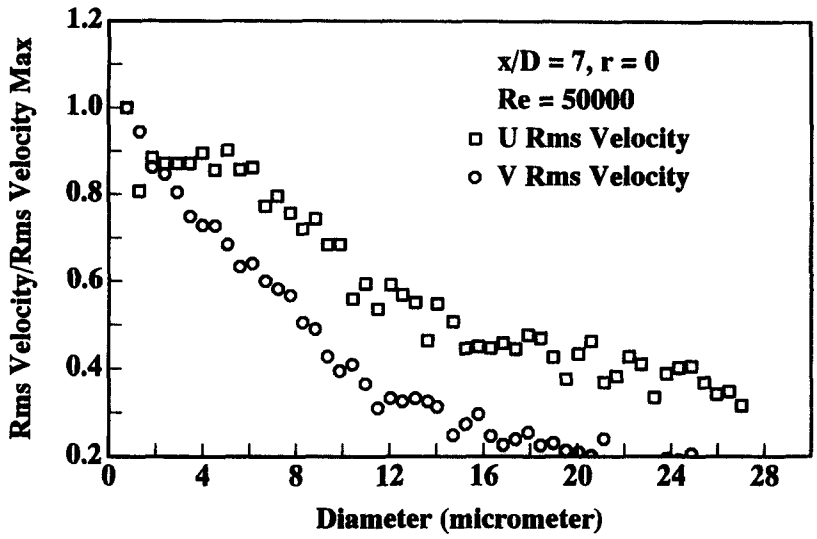


Figure 20. Plot of the normalized RMS velocities for the radial and axial velocity components as a function of the particle diameters.

coupling process was generated wherein the gas turbulence was unaffected by the particles but the particles were affected by the turbulence.

Because of space limitations, results of only one flow condition will be presented here. Complete results were presented in Bachalo *et al.* (1993). The spray drop velocities are presented for three size classes in figure 21(a), (b) and (c) for the 20 m/s run condition. A vector representation of the data was used to enable a better understanding of the flow behavior. The vectors at each point delineate the velocity averaged over 10° intervals of the flow angle with the size of the vector head

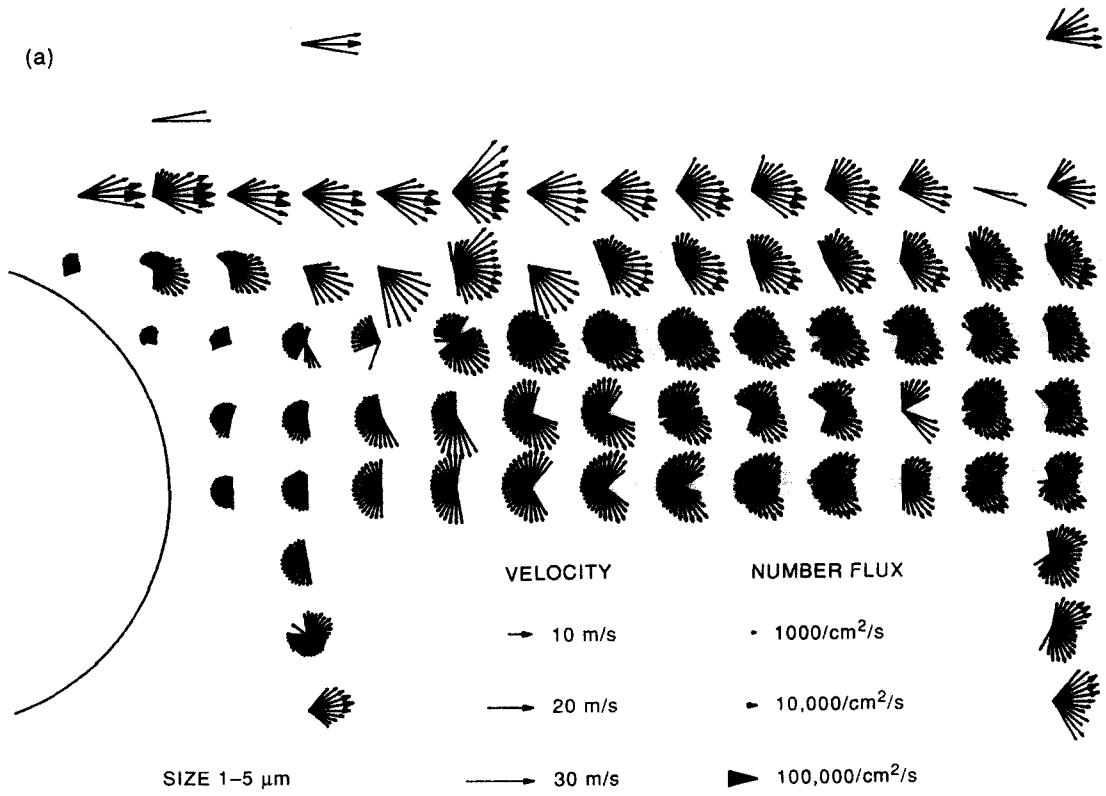


Fig. 21(a). *Caption opposite.*

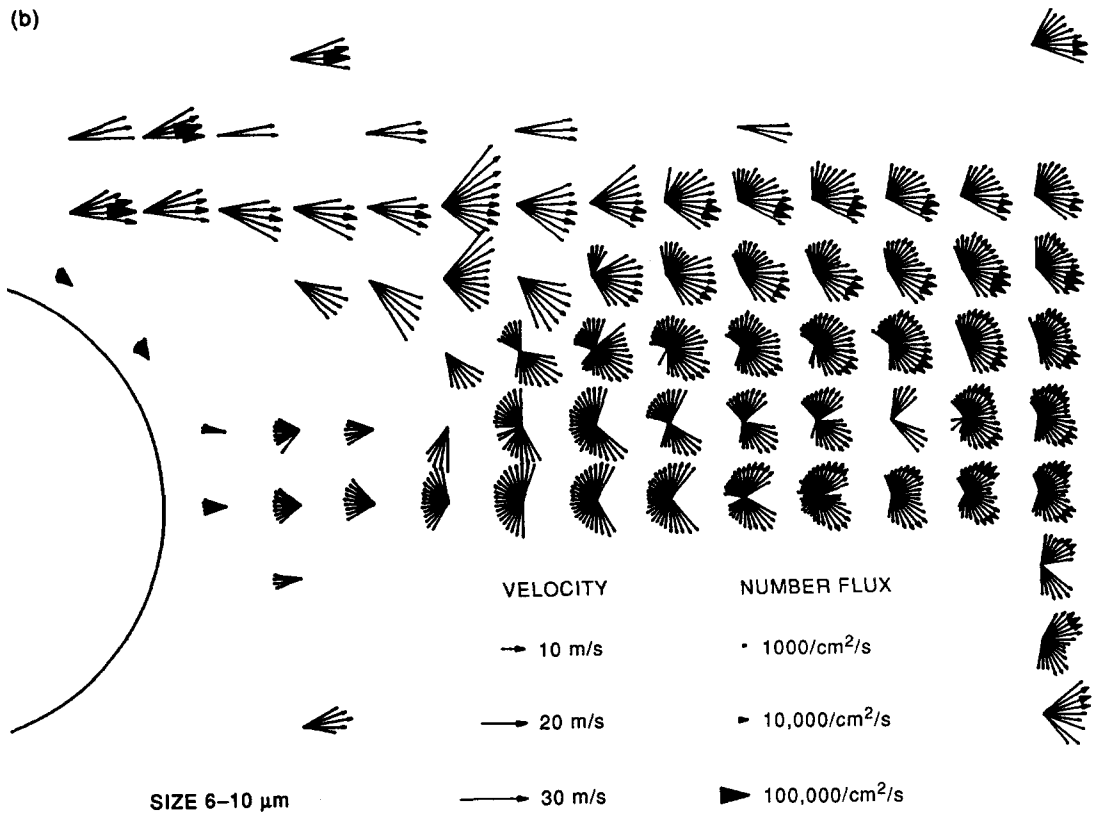


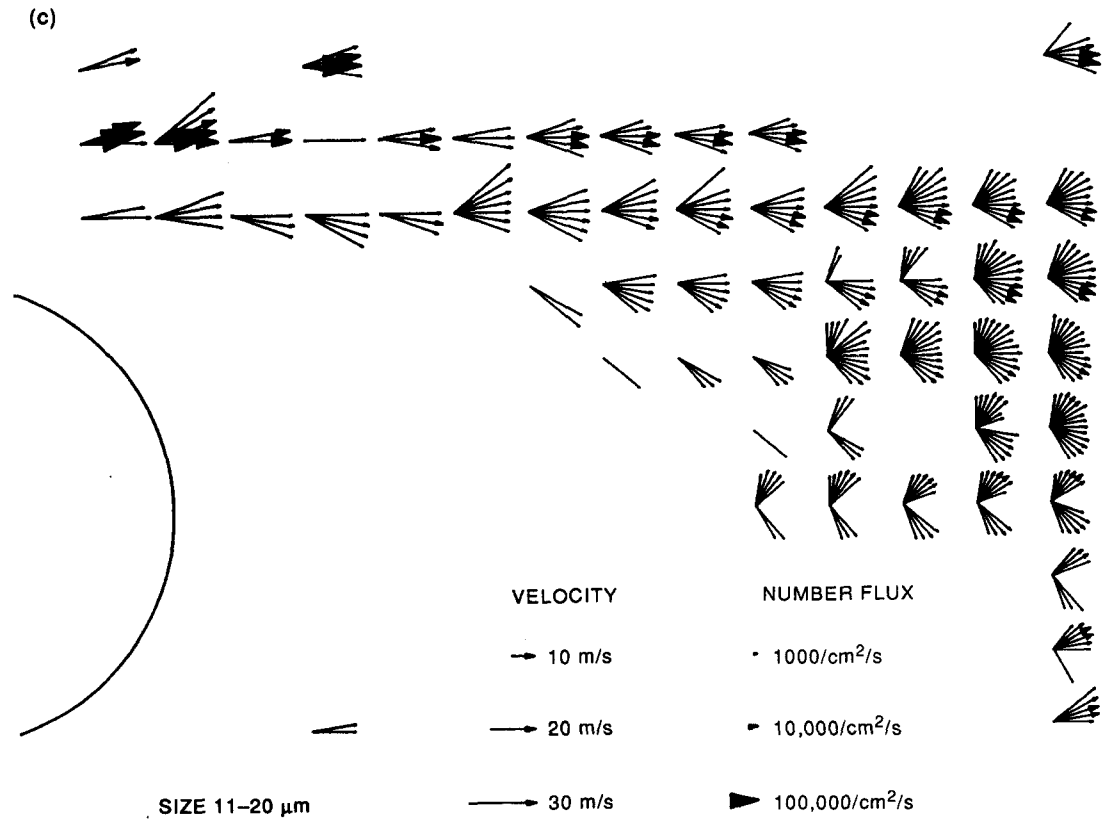


Figure 21(b) and (c)

**Figure 21. Vector plots for the free stream flow speed of 20 m/s. (a) 1–5 $\mu$m particle response to large scale eddies; (b) 6–10 $\mu$m particle response to large scale eddies; and (c) 11–20 $\mu$m particle response to large scale eddies.**

proportional to the number of velocity readings measured at each angular increment. Data were acquired over a matrix with 1 cm spacings. Since these data were time averaged, they represent the range of excursions in velocity direction and magnitude as the vortices were shed and convected downstream.

Close observation of the data will reveal that only the particles in the range from 1 to 5 $\mu$m [figure 21(a)], were able to penetrate into the near-wake of the cylinder, as seen by the vectors for this size range. The shedding frequency for the case was approx. 65 Hz. On the center line in the neighborhood of the rear stagnation point (9 cm from the trailing edge of the cylinder), the velocity vectors varied through all directions but with the maximum number of readings, as indicated by the size of the arrow heads, nearly equally distributed between the $\pm 45^{\circ}$ directions. For the reversed flow in the separated flow region, the flow direction varied from $\pm 130^{\circ}$ indicating that the flow direction varied dramatically with each shed vortex. In the outer two rows of data, the variation in the flow angle was about $\pm 45^{\circ}$.

Drops in the size range of 6–10 $\mu$m [figure 21(b)], could not follow the vortex formed near the cylinder as seen by the absence of the data in this region. The overall angular excursions of these larger drops was noticeably less than for the 1–5 $\mu$m particles. This was most evident in the velocity vectors on the center line and near to the cylinder. Figure 21(c) shows the behavior of the drops in the size range of 11–20 $\mu$m. Unfortunately, there was a much lower population of these drops in the spray. However, it is still possible to observe that the angular excursions of their velocities was quite different from the air flow as represented by the smallest drops (1–5 $\mu$m) and that few if any drops were dispersed into the near wake flow of the cylinder.

An estimation of the Stokes number could be made using the tangential drop velocity of 45 m/s and the radius of the drop trajectories, estimated at 35 cm. The Stokes numbers are approx.

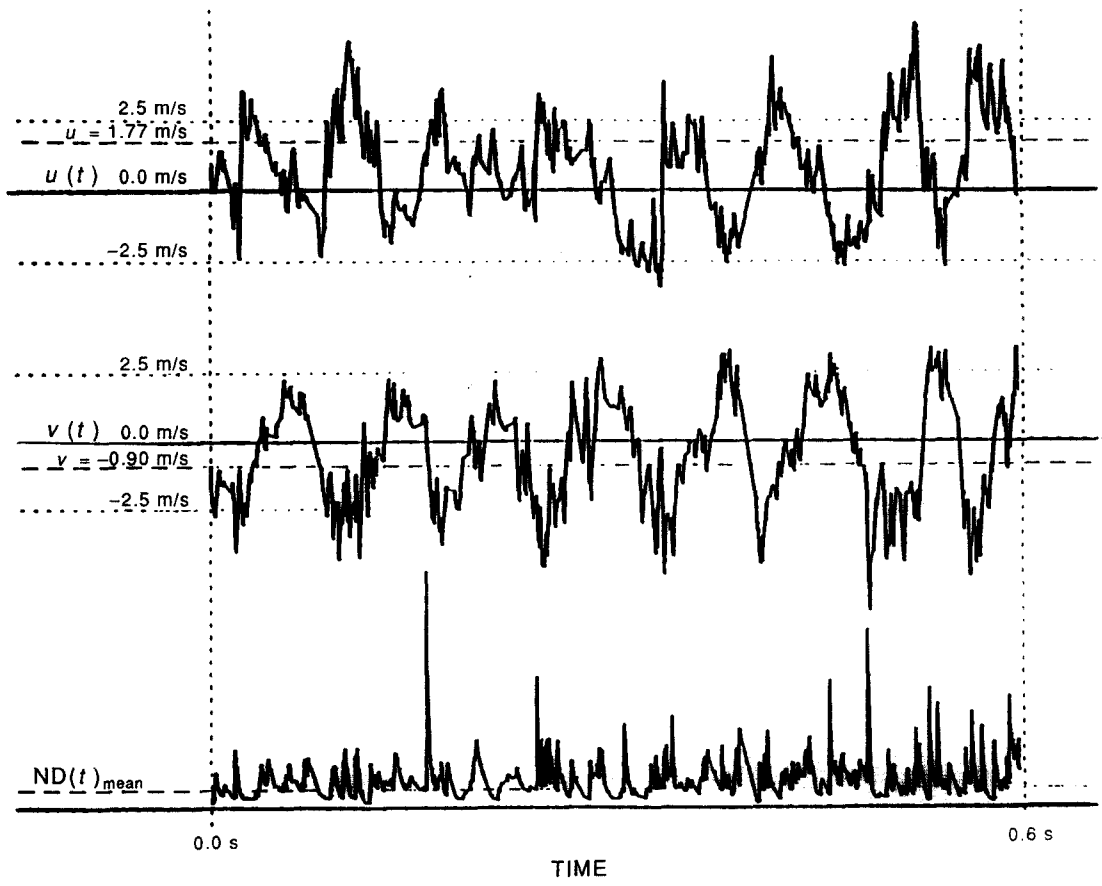


Figure 22. Time-of-arrival records for velocity and number density.

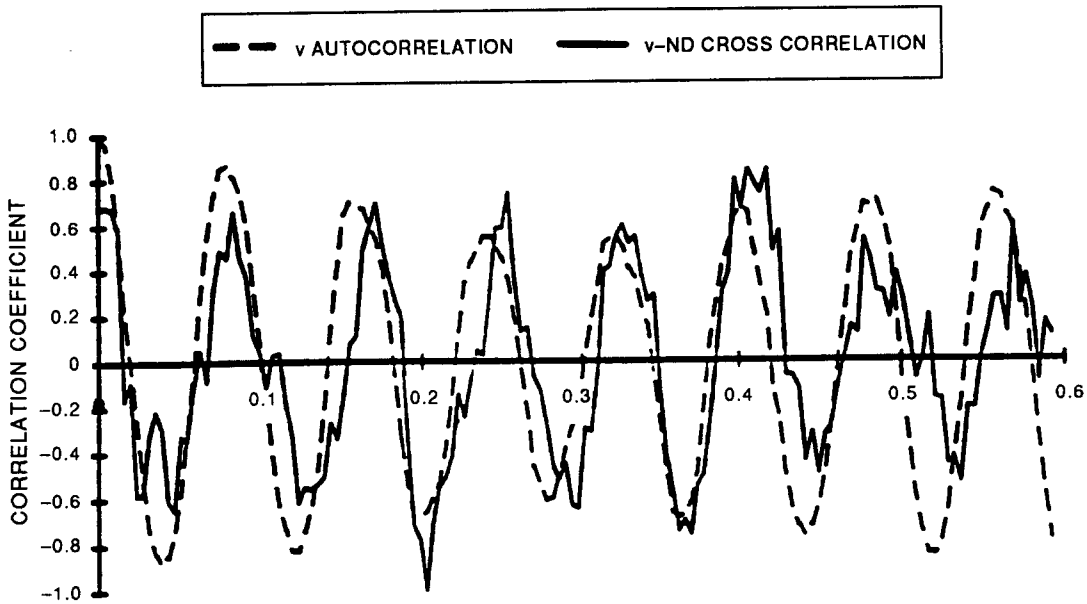


Figure 23. Cross correlation of the velocity with the number density.

St = 0.04, 0.08 and 0.16 for drop sizes of 10, 15 and 20 $\mu$m. This was consistent with the requirement that the Stokes number be 0.1 in order for particles to track the flow. Only a few drops in the size range of 11–20 $\mu$m were able to follow this radius of curvature.

A selected example of the particle time-of-arrival record is shown in figure 22 for the low speed case. Only a very small fraction of the time records consisting of 10,000 drop measurements at each location was displayed. At the station selected, there was clearly a strong periodicity in the flow velocity for both the axial and radial components resulting from the vortex shedding by the cylinder. A Fourier analysis of the time-of-arrival records was computed by breaking the time record into uniform time intervals or time slots with periods much shorter than the period of the highest frequency of interest in the flow. The velocity measurements in each time slot were taken as the average for the particles arriving in that interval. Using this approach, the resulting power spectra showed a strong peak at 12.5 Hz. As expected, the value was in very good agreement with the Strouhal number of 0.2 for the free stream velocity of 3.88 m/s.

There was also an indication of randomly formed drop clusters and voids as seen by intervals of very few readings and intervals with a high number of readings. Clearly, at this flow Reynolds number, the turbulence does not produce a uniform mixing of the drops in the flow even well downstream of the cylinder. If a Fourier analysis was applied to the particle count rate, a frequency equal to the velocity fluctuation frequency will be reported. However, one must realize that the particle arrival rate is directly proportional to the particle velocity so this result can be misleading. In order to determine whether the drop concentrations and voids resulted from the interaction with the vortex shedding frequency, the cross correlation between the velocity magnitude and the particle concentration or number density was computed. It was necessary to first compute the number density for each time increment which required division of the number of samples within the time increment by the sample volume cross section and by the velocity of the samples within the sampling time increment. The instantaneous local number density computed in this manner could be useful information for assessing local fuel concentration and the characteristics of the drop dispersion process. The local particle number density fluctuations are shown in figure 22.

An example of the cross correlation of the velocity and the drop time dependent number density fluctuations is shown in figure 23. The autocorrelation of the velocity–time record was first applied to remove uncorrelated turbulent fluctuations in the data although this was not necessary. The cross correlation with the number density showed a sinusoidal frequency at the same period as the shedding frequency. This confirmed, as may have been expected, that the large scale vortices served to convey fluid containing high concentrations of drops into the wake down stream of the cylinder. Also shown is the time history of the local particle number density superimposed on the autocorrelation of the velocity record.

## SUMMARY AND CONCLUSIONS

Experimental methods for multiphase flows have advanced significantly over the past decade. The development of the laser based diagnostics and primarily, the phase Doppler method, allows detailed measurements of the particle size and velocity as well as turbulence parameters in realistic flow facilities. In addition to the continuous phase turbulence parameters and the particle dynamics, the measurements of the mean and time varying particle number density and volume flux are also possible. However, there are some conditions under which the measurements may not be completely reliable. Developments in the instrumentation components are being made to improve on the measurement reliability in these difficult environments. Whenever the dispersed phase consists of or can be simulated with spherical particles, the phase Doppler method is clearly the method to use for the flow characterization.

If the dispersed phase consists of irregular shaped particles, it is necessary to use a particle counting technique that embodies light scatter detection in the near-forward direction. Light scattered in the forward direction is dominated by the Fraunhofer diffraction and as such, is relatively insensitive to the particle shape if axisymmetric detection is used. Past problems of reconciling uncertainty due to the particle trajectory through the Gaussian laser beam intensity profile has been solved using confocal laser beams of differing polarization or wavelength. This approach, combined with the laser Doppler velocimeter should provide a similar capability for the research on multiphase flows with irregular particles.

Some basic flow visualization methods have also been reviewed. Flow visualization is an invaluable tool for obtaining a qualitative understanding of the flow phenomena. There are numerous techniques that have been used and that are described in the literature from the simple dye streak methods to the use of thermal streaks and interferometry. A novel method described in this review using $TiO_2$ particles appears to be a very simple and useful method for tracking particles and for observing the flow behavior in the presence of a dispersion of particles.

There is a good deal of interest in particle image velocimetry for research in fluid mechanics. Although this method has some shortcomings such as being unable to measure the third velocity component, it does provide information heretofore unavailable. The instrument could gain a great deal of value if the simultaneous particle sizing ability could be added to it.

Some examples of the measurements in turbulent two-phase flows have been presented to demonstrate the capabilities available with the advanced laser-based diagnostics. It is now possible to examine in detail, the interaction of the dispersed phase with the turbulence. The mixing and formation of particle voids and clusters may also be examined. Thus, the field of multiphase flow should be advanced as a result of these developments in the diagnostics.

## REFERENCES

ADRIAN, R. J. 1988 Statistical properties of particle image velocimetry measurements in turbulent flow. In *Laser Anemometry in Fluid Mechanics—III* (Edited by ADRIAN, R. *et al.*), pp. 115–129.

ADRIAN, R. J. 1991 Particle imaging techniques for experimental fluid mechanics. *A. Rev. Fluid Mech.* **23,** 261–304.

ADRIAN, R. J. & YAO, C. S. 1984 Development of pulsed laser velocimetry (PLV) for measurement of turbulent flow. In *Proc. Symp. Turbul.* (Edited by REED, X.), pp. 170–186.

ADRIAN, R. J., DURAO, D. F. G., DURST, F., MAEDA, M. & WHITELAW, J. H. (Eds) 1990 Application of laser techniques to fluid mechanics. In *Fifth International Symposium*, Lisbon, Portugal, 9–12 July.

ALEXANDER, D. R., WILES, J. J., SCHAUB, S. A. & SEEMAN, M. P. 1985 Effects of non-spherical drops on a phase Doppler spray analyzer. *SPIE (Society of Photo-Optical Instrumentation Engineers) Particle Sizing and Spray Analysis* **573,** 67–72.

BACHALO, W. D. 1979 Apparatus for sizing particles, droplets or the like with laser scattering. Serial No. 067116, filed 16 August 1979; awarded in 1980.

BACHALO, W. D. 1980 Method for measuring the size and velocity of spheres by dual-beam light scatter interferometry. *Appl. Opt.* **19,** 363–370.

BACHALO, W. D. 1982 Analysis and testing of a new processing method for laser light scattering interferometry. NASA Contract Report NAS 3-23684.

BACHALO, W. D. 1988 Apparatus for sizing particles, drops, bubbles or the like using laser light scattering and confocal beams. Awarded in 1989.

BACHALO, W. D. 1989 Improved method for measuring the size and velocity of spherical particles using the phase and intensity of the scattered light.

BACHALO, W. D. & HOUSER, M. J. 1984a Phase Doppler spray analyzer for simultaneous measurements of drop size and velocity distributions. *Opt. Engng* **23,** 583.

BACHALO, W. D. & HOUSER, M. J. 1984b Analysis and testing of a new method for drop size measurement using light scatter interferometry. NASA Contract Report 174636, NASA Lewis Research Center.

BACHALO, W. D. & HOUSER, M. J. 1984c Development of the phase Doppler spray analyzer for liquid drop size and velocity characterizations. AIAA Paper No. 84-1199.

BACHALO, W. D. & SANKAR, S. V. 1988 Analysis of the light scattering interferometry for spheres larger than the wavelength. In *Proceedings of 4th Int. Symposium on Applications of Laser Anemometry to Fluid Mechanics*, Lisbon, Portugal.

BACHALO, W. D., RUDOFF, R. C. & BRENA DE LA ROSA, A. 1988 Mass flux measurements of a high number density spray system using the phase Doppler particle analyzer. Presented at the *AIAA 26th Aerospace Sciences Meeting*, 11–14 Jan., Reno, NV.

BACHALO, W. D., RUDOFF, R. C. & HOUSER, M. J. 1987 Laser velocimetry in turbulent flow fields: particle response. Presented at the *AIAA 25th Aerospace Sciences Meeting*, January, Reno, NV.

BACHALO, W. D., RUDOFF, R. C. & SANKAR, S. V. 1988 Time-resolved measurements of spray and velocity. In *Liquid Particle Size Measurement Techniques* (Edited by HIRLEMAN, BACHALO, W. D. & FELTON), ASTM STP1083, pp. 209–224.

BACHALO, W. D., RUDOFF, R. C. & ZHU, J. Y. 1992 An investigation of particle response in turbulent flows. Presented as a Keynote Lecture at the *Fifth Asian Congress of Fluid Mechanics*, 10–14 August, Daejon, Korea.

BACHALO, W. D., BACHALO, E. J., HANSCOM, J. & SANKAR, S. V. 1993 An investigation of spray interaction with large-scale eddies. Presented at the *AIAA 31st Aerospace Sciences Meeting*, 11–14 Jan., Reno, NV, paper AIAA 93-0697.

BERNAL, L. P. & SCHERER, J. 1993 HPIV measurements in vortical flows. In *ASME Fluids Engineering Conference, Holographic Particles Image Velocimetry*, paper 8.

BESSEM, J. M., BOOIJ, R., GODEFROY, H. W. H. E., DE GROOT, P. J., KRISHNA PRASAD, K., DE MUL, F. F. M. & NIJHOF, E. J. (Eds) 1993 *Laser Anemometry: Advances and Applications—Proceedings of the Fifth International Conference*, Proc. SPIE 2052.

BROWN, D. J. & HUTCHINSON, P. 1979 The interaction of solid or liquid particles and turbulent fluid flow fields—a numerical simulation. *J. Fluids Engng* **101,** 265–269.

CRANE, R. 1969 Interference phase measurement. *Appl. Opt.* **8,** 538.

DODGE, L. G., RHODES, D. J. & REITZ, R. D. 1986 Comparison of drop-size measurement techniques in fuel sprays: Malvern laser diffraction and aerometrics phase/Doppler. Presented at the *Spring 1986 Meeting of the Central States Section/The Combustion Institute*, 5–6 May, NASA Lewis Research Center.

DRING, R. P. & SUO, M. 1978 Particle trajectories in swirling flows. *J. Energy* **2,** 232–237.

DURST, F., MELLING, A. & WHITELAW, J. H. 1981 *Principals and Practice of Laser-Doppler Anemometry*, 2nd edn. Academic Press, London.

DURST, F. 1982 Combined measurements of particle velocities, size distributions, and concentration. *Trans. ASME, J. Fluids Engng* **104,** 284–296.

EDWARDS, C. F. & MARX, K. D. 1992 Analysis of the ideal phase-Doppler system: limits imposed by the single-particle constraint. *Atomization Sprays* **2,** 319–366.

EDWARDS, C. F. & MARX, K. D. 1994 Theory and measurement of the multi-point statistics of sprays. Submitted to *Recent Advances in Spray Combustion, AIAA Progress Series.*

FARMER, W. M. 1972 Measurement of particle size, number density, and velocity using a laser interferometer. *Appl. Opt.* No. 11.

GEBHART, J. & ANSELM, A. 1988 *Effect of Particle Shape on the Response of Single Particle Optical*

*Counters, Optical Particle Sizing: Theory and Practice* (Edited by GOUESBET, G. & GREHAN, G.), pp. 393–409. Plenum Press, New York.

GOUESBET, G., MAHEU, B. & GRÉHAN, G. 1988 Light scattering from a sphere arbitrarily located in a Gaussian beam using a Bromwich formulation. *J. Opt. Soc. Am.* **5,** 1427.

GOUESBET, G., GREHAN, G. & MAHEU, B. 1990 Localized interpretation to compute all coefficients $g_n^m$ in the generalized Lorenz–Mie theory. *J. Opt. Soc. Am. A* **7,** 998–1007.

GREHAN, G., GOUESBET, G., NAQWI, A. & DURST, F. 1994 Particle trajectory effects in phase Doppler systems: computations and experiments. Submitted to *Int. J. Multiphase Flow.*

HANCOCK, R. D., JACKSON, T. A. & NEJAD, A. S. 1992 Technique for visualizing vaporlines emanating from water drops. *Appl. Opt.* **31,** 20.

HARDALUPAS, Y., TAYLOR, A. M. K. P. & WHITELAW, J. H. 1992 Particle dispersion in a vertical round sudden expansion flow. *Phil. Trans. R. Soc. Lond.*

HINSCH, K. D. 1993 The many dimensions of optical flow diagnostics. In *Laser Anemometry: Advances and Applications—Proceedings of the Fifth International Conference* (Edited by BESSEM, J. M. *et al.*), Proc. SPIE 2052, pp. 63–78.

HINZE, J. O. 1947–1948 Forced deformations of viscous liquid droplets. *Appl. Sci. Res.* **A1,** 263–272.

HINZE, J. O. 1972 Turbulent fluid and particle interaction. In *Progress in Heat and Mass Transfer*, Vol. 6, Pergamon Press, New York.

HOFELDT, D. L. 1991 Instantaneous imaging diagnostics for measuring particles sizes and spatial distributions over extended regions in two-phase flows. Ph.D. dissertation, Department of Mechanical Engineering, Stanford University, Stanford, CA, U.S.A.

HUMPHRIES, W. & VINCENT, J. H. 1978 The transport of airborne dusts in the wakes of bluff bodies. *Chem. Engng Sci.* **33,** 1141–1146.

IBRAHIM, K. M., WERTHIMER, G. D. & BACHALO, W. D. 1990 Signal processing considerations for laser Doppler & phase Doppler applications. In *5th International Symposium on the Application of Laser Techniques to Fluid Mechanics*, July, Lisbon, Portugal.

IBRAHIM, K. M. & BACHALO, W. D. 1992 The significance of the Fourier analysis in signal detection and processing in laser Doppler & phase Doppler applications. In *6th International Symposium on the Application of Laser Techniques to Fluid Mechanics*, July, Lisbon, Portugal.

JONES, A. R. 1988 Fraunhofer diffraction by random irregular particles. In *Optical Particle Sizing: Theory and Practice* (Edited by GOUESBET, G. & GREHAN, G.), pp. 301–310. Plenum Press, New York.

KILLINGER, R. T. & ZERULL, R. H. 1988 Effects of shape and orientation to be considered for optical particle sizing. In *Optical Particle Sizing: Theory and Practice* (Edited by GOUESBET, G. & GREHAN, G.), pp. 419–429. Plenum Press, New York.

MAEDA, M., HISHIDA, K., SEKINE, M. & WATANABE, N. 1986 Measurements on spray jet using LDV system with particle sizing discrimination. In *Proceedings, Third International Symposium on Applications of Laser Anemometry to Fluid Mechanics*, 7–9 July, Lisbon, Portugal, paper 20.3.

MCDONELL, V. G., CAMERON, C. D. & SAMUELSEN, G. S. 1987 Symmetry assessment of a gas turbine air-blast atomizer. In *AIAA/SAE/ASME/ASEE 23rd Joint Propulsion Conference*, San Diego, CA, U.S.A.

MODARRESS, D., WUERER, J. & ELGOBASHI, S. 1982 An experimental study of a turbulent round two-phase jet. AIAA Paper 82-0964.

NYGA, R., SCHMITZ, E. & LAUTERBORN, W. 1990 In-line holography with a frequency doubled Nd:YAG laser for particle size analysis. *Appl. Opt.* **29,** 3365–3368.

O'HERN, T. J. & GORE, R. A. (Eds) 1991 *Experimental Techniques in Multiphase Flows*, ASME, FED, Vol. 125.

ROTH, N., ANDERS, K. & FROHN, A. 1993 Measurement of the rainbow position using a PSD-sendor. In *Third International Congress on Optical Particle Sizing*, 23–26 Aug., Yokohama, Japan.

RUDOFF, R. C., KAMEMOTO, D. Y. & BACHALO, W. D. 1991 Effects of turbulence and number density on the drag coefficient of droplets. Presented at the *29th AIAA Aerospace Sciences Meeting*, 7–10 Jan., Reno, NV, paper AIAA 91-0074.

SAFFMAN, M. 1986 The use of polarized light for optical particle sizing. In *Proceedings, The Third International Symposium on Applications of Laser Anemometry to Fluid Mechanics*, 18 February, Lisbon, Portugal.

SANKAR, S. V., BRENA DE LA ROSA, A., ISAKOVIC, A. & BACHALO, W. D. 1990 A technique for studying mixing in swirl combustors. Presented at the *Fifth International Symposium on the Application of Laser Techniques to Fluid Mechanics*, 9–12 July, Lisbon, Portugal.

SANKAR, S. V. & BACHALO, W. D. 1991 Response characteristics of the phase Doppler particle analyzer for sizing spherical particles larger than the wavelength. *Appl. Opt.* **30,** 1487–1496.

SANKAR, S. V., WEBER, B. J., KAMEMOTO, D. Y. & BACHALO, W. D. 1991 Sizing fine particles with the phase Doppler interferometric technique. *Appl. Opt.* **30,** 4914–4920.

SANKAR, S. V., INENAGA, A. & BACHALO, W. D. 1992 Trajectory dependent scattering in phase Doppler interferometry: minimizing and eliminating sizing errors. Presented at the *Sixth International Symposium on the Application of Laser Techniques to Fluid Mechanics*, July, Lisbon, Portugal.

SANKAR, S. V., IBRAHIM, K. M., BUERMANN, D. H., FIDRICH, M. J. & BACHALO, W. D. 1993 An integrated phase Doppler/rainbow refractometer system of simultaneous measurement of droplet size, velocity, and refractive index. Presented at the *Third International Congress on Optical Particle Sizing*, August, Japan, Yokohama.

SANKAR, S. V., IBRAHIM, K. M. & BACHALO, W. D. 1994 Coherent scattering by multiple particles in phase Doppler interferometry. In *Particle and Particle Systems Characterization*. In press.

SCHNEIDER, M., HIRLEMAN, E. D., SALEHEEN, H., CHOWDHURY, D. Q. & HILL, S. C. 1993 Rainbows and radially-inhomogeneous droplets. In *Proceedings of the Third International Congress on Optical Particle Sizing*, 23–26 August, Yokohama, Japan.

SIMO, J. A. & LIENHARD, J. H. 1991 Turbulent transport of inertial aerosols. In *27th National Heat Transfer Conference, Transport Phenomena Associated with Aerosol*, July, Minneapolis, MN, U.S.A.

SIRIGNANO, W. A. 1993 Fluid dynamics of sprays—1992 Freeman Scholar Lecture. *J. Fluids Engng* **115,** 345–378.

SMALLWOOD, G. J. 1992 A technique for two-color particle image velocimetry. Thesis submitted to Department of Mechanical Engineering, University of Ottawa, Ottawa, Ontario, Canada.

THOMPSON, B. J., WARD, J. H. & ZINKY, W. R. 1967 Application of hologram techniques for particle size analysis. *Appl. Opt.* **6,** 519–526.

THOMPSON, B. J. 1982 Holographic methods of dynamic particle measurements—current status. *Proc. Soc. Photo-Opt. Instrum. Engng* **348,** 628.

THOMPSON, B. J. 1989 Holographic methods for particle size and velocity measurement—recent advances. In *Holographic Optics II: Principals and Applications* (Edited by MORRIS, G. M.), Proc. SPIE, 1136, pp. 308–326.

TOROBIN, L. B. & GAUVIN, W. H. 1960 Fundamental aspects of solids–gas flow—Part V: the effects of fluid turbulence on the particle drag coefficient. *Can. J. Chem. Engng* **Dec.,** 189.

VAN DE HULST 1981 *Light Scattering by Small Particles*. Dover.

YEH, Y. & CUMMINS, H. Z. 1964 Localized fluid flow measurements with an HeNe laser spectrometer. *Appl. Phys. Lett.* **4,** 176–178.

ZHU, J. Y., RUDOFF, R. C., BACHALO, E. J. & BACHALO, W. D. 1993 Number density and mass flux measurements using the phase Dopplet particle analyzer in reacting and non-reacting swirling flows. Presented at the *31st Aerospace Sciences Meeting and Exhibit*, 11–14 January, Reno, NV, paper AIAA 93-0361.